Laser Physics, Vol. 14, No. 10, 2004, pp. 1342–1365.

Nonlinear Response Functions of Strongly Correlated Boson Fields: Bose–Einstein Condensates and Fractional Quantum Hall Systems

S. Choi[1], O. Berman[2], V. Chernyak[3], and S. Mukamel[1, 2]

[1] *Department of Physics and Astronomy, University of Rochester, Rochester, New York, 14627 USA*
[2] *Department of Chemistry, University of Rochester, Rochester, New York, 14627 USA*
[3] *Corning Incorporated, Process Engineering and Modeling, Corning, New York, 14831 USA*
e-mail: choi@pas.rochester.edu
Received February 18, 2004

Abstract—Nonlinear response functions of strongly correlated boson fields subject to an external perturbation are calculated. In particular, the second-order response functions and susceptibilities of finite-temperature Bose–Einstein condensates (BECs) in a one-dimensional harmonic trap driven by an external field coupled to particle density are calculated by solving the time-dependent Hartree–Fock–Bogoliubov equations. These provide additional insight into the BEC dynamics, beyond those of the linear response regime. We further demonstrate that the results directly apply to electron liquids in the fractional quantum Hall effect regime that can be mapped onto an effective boson system coupled to a Chern–Simons gauge field.

1. INTRODUCTION

The study of strongly correlated systems has been one of the most vigorous areas of research in condensed-matter physics. Some notable examples include Bose–Einstein condensation and associated phenomena, such as superfluidity and superconductivity [1], and the quantum Hall effect in two-dimensional electron systems [2]. A useful tool for the study of such complex, correlated many-body systems is provided by linear and nonlinear response functions to external perturbations. The linear response provides an adequate description of systems subjected to weak external perturbations. For stronger perturbations, nonlinear effects contained in the higher order terms in the perturbation series in the driving field may not be ignored and provide useful insights. The nonlinear response formalism has had remarkable successes in the field of nonlinear optics, where the coherent response of semiconductor metals and molecular systems to multiple laser fields is routinely analyzed in terms of multitime correlation functions [3, 4].

It is by now well known that strong similarities exist between nonlinear optics and the dynamics of Bose-Einstein condensates (BECs) owing to the intrinsic interatomic interactions in Bose condensates. Previous work done in this area includes the demonstration of four-wave mixing in zero-temperature BEC using the Gross–Pitaevskii equation (GPE) [5]. We have recently studied an externally driven, finite-temperature BEC described by the time-dependent Hartree–Fock–Bogoliubov (TDHFB) equations [6]. A systematic procedure was outlined for solving these equations perturbatively in the applied external field, and position-dependent linear response functions and susceptibilities were calculated [7]. In this paper, we extend the formalism of [7] to obtain the nonlinear response of BEC and fractional quantum Hall system.

Several dynamical theories exist for finite-temperature BEC that take into account higher order collision processes. They include the Hartree–Fock–Bogoliubov (HFB) theory [8–11], the time-dependent Bogoliubov–de Gennes equations [12], quantum kinetic theory [13–18], and stochastic methods [19–23]. The TDHFB theory is a self-consistent theory of BEC in the collisionless regime that progresses logically from the Gross–Pitaevskii equation by taking into account higher order correlations of noncondensate operators. Although TDHFB neglects higher order correlations included in the various quantum kinetic theories, the TDHFB equations are valid at very low temperatures near zero, even down to the zero-temperature limit, and are far simpler than the kinetic equations, which can only be solved under certain approximations [16]. Another attractive feature of TDHFB from a purely pragmatic point of view is that the fermionic version of the theory has already been well developed in nuclear physics [8]. We therefore work at the TDHFB level in this paper, and our approach draws upon the analogy with the time-dependent Hartree–Fock (TDHF) formalism developed for nonlinear optical response of many-electron systems [24].

Another important, strongly correlated many-body system that we consider in this paper is the two-dimensional (2D) electron system in the fractional quantum Hall effect (FQHE) regime [2]. The FQHE for a 2D electron gas in a strong, perpendicular, external magnetic field has been observed through the quantization of the Hall dc conductivity $\sigma_H(\nu)$ as a function of the

filling factor $\nu \equiv (2\pi n)/(m\omega_c)$, where n is the mean 2D density of the electrons, $\omega_c = eB/mc$ is the cyclotron frequency, and B is the magnetic field; e is the electron charge (we set $c = 1$ and $\hbar = 1$). At $\nu = 1/(2k + 1)$, where k is an integer $k = 1, 2, \ldots$, $\sigma_H(\nu)$ varies in discrete steps and is given by $\sigma_H(\nu) = \nu(e^2/2\pi)$.

Nonlinear response functions for FQHE systems have not been extensively studied so far. We demonstrate in this paper that the FQHE is, in fact, formally related to a BEC driven by an external potential, allowing the results obtained for BEC to be carried over directly to FQHE. The nonlinear response of a 2D electron system in the FQHE regime at fixed temperature is important, since it can be used to distinguish between the Fermi liquid and Luttinger chiral liquid behavior [25].

It has been shown that, for $\nu = 1/(2k + 1)$, the original 2D fermion problem can be mapped into a boson system coupled to a Chern–Simons gauge field added to the time-independent external magnetic field, where the original fermion system and the boson system have the same charge density and Hall conductivity [26–28]. The static Hall conductivity (xy component of the conductivity tensor) calculated for this boson system, $\sigma_H = \nu(e^2/2\pi)$, coincides with the conductivity obtained by using Laughlin's ansatz for the many-electron wave function [29]. For an even inverse filling number $\nu = 1/(2k)$, the original fermion problem is mapped onto a composite fermion system coupled to a Chern–Simons gauge field [30]. At $\nu = 1/2$, this gauge field eliminates the external effective vector potential for the effective composite fermion system [31–33]. In this paper, we consider FQHE with the odd inverse denominator of the filling number $\nu = 1/(2k + 1)$. Using this mapping, we can apply our results based on a generalized coherent state (GCS) ansatz for the many-particle wave function of a weakly interacting effective boson system [7, 39, 40] to compute the second-order response of FQHE.

The paper is organized as follows. In Section 2, the second-order time and frequency domain response functions for an externally driven BEC are presented, including the discussion of numerical results for a condensate of 2000 atoms in a one-dimensional harmonic trap. We then show in Section 3 how the formalism may be applied for computing the second-order response for a fractional quantum Hall system. In Section 4, we conclude. More detailed derivation of the second-order response functions and susceptibilities are provided in Appendices C and D, respectively.

2. NONLINEAR RESPONSE OF AN EXTERNALLY DRIVEN BEC

2.1. Formalism

We adopt the notation of [7] throughout the paper. The Hamiltonian describing the system of an externally driven, trapped atomic BEC is given by

$$\hat{H} = \hat{H}_0 + \hat{H}'(t), \tag{1}$$

where

$$\hat{H}_0 = \sum_{ij} H_{ij}^{sp} \hat{a}_i^\dagger \hat{a}_j + \frac{1}{2}\sum_{ijkl} V_{ijkl} \hat{a}_i^\dagger \hat{a}_j^\dagger \hat{a}_k \hat{a}_l, \tag{2}$$

and

$$H'(t) = \eta \sum_{ij} E_{ij}(t) \hat{a}_i^\dagger \hat{a}_j, \tag{3}$$

with

$$E_{ij}(t) \equiv \int d^3\mathbf{r} \phi_i^*(\mathbf{r}) V_f(\mathbf{r}, t) \phi_j(\mathbf{r}). \tag{4}$$

The boson operators $\hat{a}_i^\dagger$ ($\hat{a}_i$) create (annihilate) a particle from a basis state with wave functions $\phi_i(\mathbf{r})$. The single-particle Hamiltonian H^{sp} in Eq. (2) is diagonal if the basis state $\phi_i(\mathbf{r})$ is chosen to be the eigenstates of the trap, while the symmetrized interaction matrix elements,

$$V_{ijkl} = \frac{1}{2}[\langle ij|V|kl\rangle + \langle ji|V|kl\rangle], \tag{5}$$

where

$$\langle ij|V|kl\rangle = \int d^3\mathbf{r} d^3\mathbf{r}' \phi_i^*(\mathbf{r}) \phi_j^*(\mathbf{r}') V(\mathbf{r} - \mathbf{r}') \phi_k(\mathbf{r}') \phi_l(\mathbf{r}), \tag{6}$$

describe the collision between the atoms, with $V(\mathbf{r} - \mathbf{r}')$ being a general interatomic potential. $H'(t)$ describes the effect of a general external force $V_f(\mathbf{r}, t)$ on the condensate that mimics the mechanical force applied experimentally, such as shaking of the trap [34, 35].

The dynamics of the system is calculated by solving the time-dependent Hartree–Fock–Bogoliubov (TDHFB) equations for the condensate mean field, $z_i = \langle \hat{a}_i \rangle$, the noncondensate density $\rho_{ij} = \langle \hat{a}_i^\dagger \hat{a}_j \rangle - \langle \hat{a}_i^\dagger \rangle \langle \hat{a}_j \rangle$, and the noncondensate correlations $\kappa_{ij} = \langle \hat{a}_i \hat{a}_j \rangle - \langle \hat{a}_i \rangle \langle \hat{a}_j \rangle$. These are presented in Appendix A. These nonlinear coupled equations are solved by an order-by-order expansion of the variables z_i, ρ_{ij}, and κ_{ij}; at each order, the resulting equations to be solved become linear [7]. It is found that the sequence of linear equations to be solved has the general form

$$i\hbar \frac{d\vec{\psi}^{(n)}(t)}{dt} = \mathcal{L}^{(n)} \vec{\psi}^{(n)}(t) + \lambda^{(n)}(t), \tag{7}$$

where we have denoted the set of nth-order variables $z_i^{(n)}$, $\rho_{ij}^{(n)}$, and $\kappa_{ij}^{(n)}$ as a $2N(2N + 1) \times 1$ column vector in the Liouville space notation, where N is the number of basis states used, $\vec{\psi}^{(n)}(t) = [\vec{z}^{(n)}(t), \vec{z}^{(n)*}(t), \vec{\rho}^{(n)}(t),$

$\vec{\kappa}^{(n)}(t)$, $\vec{\rho}^{(n)*}(t)$, $\vec{\kappa}^{(n)*}(t)]^T$, and the $2N(2N+1) \times 2N(2N+1)$ matrix $\mathcal{L}^{(n)}$ is the nth-order Liouville operator obtained from the TDHFB equations [7]. The matrices $\mathcal{L}^{(n)}$ for all orders $n > 0$ are identical, i.e., $\mathcal{L}^{(1)} \equiv \mathcal{L}^{(2)} \equiv \ldots \equiv \mathcal{L}^{(n)}$, so that only the matrices $\mathcal{L}^{(0)}$ and $\mathcal{L}^{(1)}$ are required to be calculated. $\mathcal{L}^{(0)}$ and $\mathcal{L}^{(1)}$ are presented in Appendix B. The formal solution to Eq. (7) is

$$\vec{\psi}^{(n)}(t) = \frac{1}{i\hbar}\int_0^t \exp\left[-\frac{i}{\hbar}\mathcal{L}^{(n)}(t-t')\right]\lambda^{(n)}(t')dt'. \quad (8)$$

In the frequency domain, the solution to Eq. (7) takes the form

$$\vec{\psi}^{(n)}(\omega) = \frac{1}{\omega - \mathcal{L}^{(n)}}\lambda^{(n)}(\omega), \quad (9)$$

where $\vec{\psi}^{(n)}(\omega)$ and $\lambda^{(n)}(\omega)$ are the Fourier transforms of $\vec{\psi}^{(n)}(t)$ and $\lambda^{(n)}(t)$, respectively.

For the zeroth order ($n = 0$), we obtain the time-independent HFB equations (TIHFB)

$$\mathcal{L}^{(0)}\vec{\psi}^{(0)}(t) = 0, \quad (10)$$

while, for the first order ($n = 1$), the equation solved is Eq. (7) with $\lambda^{(1)}(t)$ being a $2N(2N+1) \times 1$ vector $\zeta(t)$ calculated in [7]; $\zeta(t)$ is also presented in Appendix B.

Once the nth-order solution to TDHFB is found, we can proceed to define the nth-order response functions. The physical significance of the response functions becomes more transparent when the nth-order solutions $\alpha^{(n)}$, where α is one of the variables z, ρ, or κ, are expressed in real space. We therefore introduce the position-dependent variables written in terms of the trap eigenstate basis:

$$z^{(n)}(\mathbf{r}, t) = \sum_j z_j^{(n)}(t)\phi_j(\mathbf{r}), \quad (11)$$

$$\rho^{(n)}(\mathbf{r}, t) = \sum_{ij} \rho_{ij}^{(n)}(t)\phi_i^*(\mathbf{r})\phi_j(\mathbf{r}), \quad (12)$$

$$\kappa^{(n)}(\mathbf{r}, t) = \sum_{ij} \kappa_{ij}^{(n)}(t)\phi_i(\mathbf{r})\phi_j(\mathbf{r}). \quad (13)$$

Real-space noncondensate density and noncondensate correlations are, in general, nonlocal functions of two spatial points $\rho(\mathbf{r}', \mathbf{r})$ and $\kappa(\mathbf{r}', \mathbf{r})$. We consider the $\mathbf{r} = \mathbf{r}'$ case in this paper, as this is most physically accessible. Measuring these quantities with $\mathbf{r} \neq \mathbf{r}'$ involves observing atomic correlations, which is far more difficult than for photonic counterparts, since, for a matter wave, merely implementing individual components, such as beam splitters and mirrors, requires a large-scale experimental effort. The position-dependent nth-order solution $\vec{\psi}^{(n)}(\mathbf{r}, t) \equiv [\vec{z}^{(n)}(\mathbf{r}, t), \vec{z}^{(n)*}(\mathbf{r}, t), \vec{\rho}^{(n)}(\mathbf{r}, t), \vec{\kappa}^{(n)}(\mathbf{r}, t), \vec{\rho}^{(n)*}(\mathbf{r}, t), \vec{\kappa}^{(n)*}(\mathbf{r}, t)]^T$ can be defined in the Liouville space notation from relations (11)–(13) by introducing a $2N(2N+1) \times 2N(2N+1)$ square matrix $\tilde{\Upsilon}(\mathbf{r})$:

$$\vec{\psi}^{(n)}(\mathbf{r}, t) \equiv \tilde{\Upsilon}(\mathbf{r})\vec{\psi}^{(n)}(t), \quad (14)$$

where

$$\tilde{\Upsilon}(\mathbf{r}) = \mathrm{diag}[\tilde{\phi}(\mathbf{r}), \tilde{\phi}^*(\mathbf{r}), \Phi_\rho(\mathbf{r}), \Phi_\kappa(\mathbf{r}), \Phi_\rho^*(\mathbf{r}), \Phi_\kappa^*(\mathbf{r})]. \quad (15)$$

Here, "diag[…]" denotes that $\tilde{\Upsilon}(\mathbf{r})$ is a block diagonal square matrix made of $N \times N$ blocks $\tilde{\phi}(\mathbf{r})$, $\tilde{\phi}^*(\mathbf{r})$ and $N^2 \times N^2$ blocks $\Phi_\rho(\mathbf{r})$, $\Phi_\kappa(\mathbf{r})$, $\Phi_\rho^*(\mathbf{r})$, $\Phi_\kappa^*(\mathbf{r})$. $\tilde{\phi}(\mathbf{r})$ is itself a diagonal matrix with the ith diagonal element given by the basis states $\phi_i(\mathbf{r})$, and $\Phi_\rho(\mathbf{r})$ and $\Phi_\kappa(\mathbf{r})$ are also diagonal matrices whose ijth diagonal element is given by $[\Phi_\rho(\mathbf{r})]_{ij,\,ij} = \phi_i^*(\mathbf{r})\phi_j(\mathbf{r})$, and $[\Phi_\kappa(\mathbf{r})]_{ij,\,ij} = \phi_i(\mathbf{r})\phi_j(\mathbf{r})$, respectively. Individual real-space variables $z^{(n)}(\mathbf{r}, t)$, $\rho^{(n)}(\mathbf{r}, t)$, and $\kappa^{(n)}(\mathbf{r}, t)$ are then obtained by summing over the appropriate elements of the vector $\vec{\psi}^{(n)}(\mathbf{r}, t)$:

$$\begin{aligned} z^{(n)}(\mathbf{r}, t) &= \sum_{i=1}^{n} \vec{\psi}_i^{(n)}(\mathbf{r}, t), \\ \rho^{(n)}(\mathbf{r}, t) &= \sum_{i=2n+1}^{2n+n^2} \vec{\psi}_i^{(n)}(\mathbf{r}, t), \\ \kappa^{(n)}(\mathbf{r}, t) &= \sum_{i=2n+n^2+1}^{2n+2n^2} \vec{\psi}_i^{(n)}(\mathbf{r}, t). \end{aligned} \quad (16)$$

The position-dependent second-order ($n = 2$) response function $K_\alpha^{(2)}(t, t_1, t_2, \mathbf{r}, \mathbf{r}_1, \mathbf{r}_2)$ is defined as follows:

$$\alpha^{(2)}(\mathbf{r}, t) = \int K_\alpha^{(2)}(t, t_1, t_2, \mathbf{r}, \mathbf{r}_1, \mathbf{r}_2), V_f(\mathbf{r}_1, t_1)V_f(\mathbf{r}_2, t_2)dt_1dt_2d\mathbf{r}_1d\mathbf{r}_2, \quad (17)$$

where $\alpha^{(2)}(\mathbf{r}, t)$ are second-order solutions, $\alpha = z, \rho, \kappa$. The second-order response functions for the condensate, the noncondensate density, and the correlation that

we use in our numerical calculations are given by the following expressions:

$$K_z^{(2)}(t, t_1, t_2, \mathbf{r}, \mathbf{r}_1, \mathbf{r}_2) = \sum_{i=1}^{N} [\tilde{\Upsilon}(\mathbf{r})(\vec{K}_I^{(2)}(t, t_1, t_2, \mathbf{r}_1, \mathbf{r}_2) + \vec{K}_{II}^{(2)}(t, t_1, t_2, \mathbf{r}_1, \mathbf{r}_2))]_i, \quad (18)$$

$$K_\rho^{(2)}(t, t_1, t_2, \mathbf{r}, \mathbf{r}_1, \mathbf{r}_2) = \sum_{i=2N+1}^{2N+N^2} [\tilde{\Upsilon}(\mathbf{r})(\vec{K}_I^{(2)}(t, t_1, t_2, \mathbf{r}_1, \mathbf{r}_2) + \vec{K}_{II}^{(2)}(t, t_1, t_2, \mathbf{r}_1, \mathbf{r}_2))]_i, \quad (19)$$

$$K_\kappa^{(2)}(t, t_1, t_2, \mathbf{r}, \mathbf{r}_1, \mathbf{r}_2) = \sum_{i=2N+N^2+1}^{2N+2N^2} [\tilde{\Upsilon}(\mathbf{r})(\vec{K}_I^{(2)}(t, t_1, t_2, \mathbf{r}_1, \mathbf{r}_2) + \vec{K}_{II}^{(2)}(t, t_1, t_2, \mathbf{r}_1, \mathbf{r}_2))]_i, \quad (20)$$

where $2N(2N+1) \times 2N(2N+1)$ matrix $\tilde{\Upsilon}(\mathbf{r})$ was defined in Eq. (15) and the $2N(2N+1) \times 1$ vectors $\vec{K}_I^{(2)}$ and $\vec{K}_{II}^{(2)}$ are defined:

$$\vec{K}_I^{(2)}(t, t_1, t_2, \mathbf{r}_1, \mathbf{r}_2) = \mathcal{U}(t-t_1)\tilde{\Phi}(\mathbf{r}_1)\mathcal{U}(t_1-t_2)\tilde{\Phi}(\mathbf{r}_2)\vec{\psi}^{(0)}, \quad (21)$$

$$\vec{K}_{II}^{(2)}(t, t_1, t_2, \mathbf{r}_1, \mathbf{r}_2) = \int_0^t d\tau \mathcal{U}(t-\tau)\vec{\Xi}_K(\tau - t_1, \tau - t_2, \mathbf{r}_1, \mathbf{r}_2), \quad (22)$$

where

$$\mathcal{U}(t-t') \equiv \exp\left[-\frac{i}{\hbar}\mathcal{L}^{(2)}(t-t')\right], \quad (23)$$

and

$$\tilde{\Phi}(\mathbf{r}') = \mathrm{diag}[\Phi(\mathbf{r}'), \Phi^*(\mathbf{r}'), \Phi^{(-)}(\mathbf{r}'), \Phi^{(+)}(\mathbf{r}'), \Phi^{(-)*}(\mathbf{r}'), \Phi^{(+)*}(\mathbf{r}')]. \quad (24)$$

$\tilde{\Phi}(\mathbf{r}')$ is therefore a $2N(2N+1) \times 2N(2N+1)$ block diagonal square matrix with the blocks consisting of $N \times N$ square matrices $[\Phi(\mathbf{r})]_{ij} = \phi_i^*(\mathbf{r})\phi_j(\mathbf{r})$ and $N^2 \times N^2$ square matrices $[\Phi^{(\pm)}(\mathbf{r})]_{ij,mn} = \phi_i^*(\mathbf{r})\phi_m(\mathbf{r})\delta_{jn} \pm \phi_n^*(\mathbf{r})\phi_j(\mathbf{r})\delta_{im}$. The vector $\vec{\Xi}_K$ of Eq. (22) may be written

$$\vec{\Xi}_K = [\mathcal{L}_K, \mathcal{L}_K^*, \mathcal{R}_K, \mathcal{K}_K, \mathcal{R}_K^*, \mathcal{K}_K^*]^T, \quad (25)$$

with the $N \times 1$ matrix $\mathcal{L}_K$ and $N^2 \times 1$ matrices $\mathcal{R}_K$, $\mathcal{K}_K$ given in Appendix C (Eqs. (C.6)–(C.10)).

Having found the time domain response $K_\alpha^{(2)}(t, t_1, t_2, \mathbf{r}, \mathbf{r}_1, \mathbf{r}_2)$, the second-order susceptibility is obtained by a Fourier transform to the frequency domain:

$$K_\alpha^{(2)}(\Omega, \Omega_1, \Omega_2, \mathbf{r}, \mathbf{r}_1, \mathbf{r}_2) = \int_0^\infty dt \int_0^\infty dt_1 \int_0^\infty dt_2 \times K_\alpha^{(2)}(t, t_1, t_2, \mathbf{r}, \mathbf{r}_1, \mathbf{r}_2) \exp(i\Omega t + i\Omega_1 t_1 + i\Omega_2 t_2). \quad (26)$$

The final expression for the susceptibility used in our numerical calculations is given for the condensate, the noncondensate density, and the noncondensate correlations in the following equations:

$$K_z^{(2)}(-\Omega_1 - \Omega_2; \Omega_1, \Omega_2, \mathbf{r}, \mathbf{r}_1, \mathbf{r}_2) = \sum_{i=1}^{N} [\tilde{\Upsilon}(\mathbf{r})(\vec{K}_I^{(2)}(\Omega_1, \Omega_2, \mathbf{r}_1, \mathbf{r}_2) + \vec{K}_{II}^{(2)}(\Omega_1, \Omega_2, \mathbf{r}_1, \mathbf{r}_2))]_i, \quad (27)$$

$$K_\rho^{(2)}(-\Omega_1 - \Omega_2; \Omega_1, \Omega_2, \mathbf{r}, \mathbf{r}_1, \mathbf{r}_2) = \sum_{i=2N+1}^{2N+N^2} [\tilde{\Upsilon}(\mathbf{r})(\vec{K}_I^{(2)}(\Omega_1, \Omega_2, \mathbf{r}_1, \mathbf{r}_2) + \vec{K}_{II}^{(2)}(\Omega_1, \Omega_2, \mathbf{r}_1, \mathbf{r}_2))]_i, \quad (28)$$

$$K_\kappa^{(2)}(-\Omega_1 - \Omega_2; \Omega_1, \Omega_2, \mathbf{r}, \mathbf{r}_1, \mathbf{r}_2) = \sum_{i=2N+N^2+1}^{2N+2N^2} [\tilde{\Upsilon}(\mathbf{r})(\vec{K}_I^{(2)}(\Omega_1, \Omega_2, \mathbf{r}_1, \mathbf{r}_2) + \vec{K}_{II}^{(2)}(\Omega_1, \Omega_2, \mathbf{r}_1, \mathbf{r}_2))]_i, \quad (29)$$

where

$$\vec{K}_I^{(2)}(\Omega_1, \Omega_2, \mathbf{r}, \mathbf{r}_1, \mathbf{r}_2) = -\frac{1}{4\pi^2}\tilde{\Upsilon}(\mathbf{r})\mathcal{U}(\Omega_1 + \Omega_2)\tilde{\Phi}(\mathbf{r}_1)\mathcal{U}(\Omega_2)\tilde{\Phi}(\mathbf{r}_2)\vec{\psi}^{(0)}, \quad (30)$$

and

$$\vec{K}_{II}^{(2)}(\Omega_1, \Omega_2, \mathbf{r}, \mathbf{r}_1, \mathbf{r}_2) = -\frac{1}{8\pi^3 i}\tilde{\Upsilon}(\mathbf{r})\mathcal{U}(\Omega_1 + \Omega_2)\vec{\Xi}_K(\Omega_1, \Omega_2, \mathbf{r}_1, \mathbf{r}_2). \quad (31)$$

Here, $\tilde{\Upsilon}(\mathbf{r})$ and $\tilde{\Phi}(\mathbf{r})$ are as defined in Eqs. (15) and (24) and

$$\mathcal{U}(\omega) \equiv \frac{1}{\omega - \mathcal{L}^{(2)} + i\epsilon}. \tag{32}$$

In addition, the vector $\vec{\Xi}_K(\Omega_1, \Omega_2, \mathbf{r}_1, \mathbf{r}_2)$ of Eq. (31) may be written as

$$\vec{\Xi}_K(\Omega_1, \Omega_2, \mathbf{r}_1, \mathbf{r}_2) = \left[\tilde{\mathcal{X}}_K, \tilde{\mathcal{X}}_K^*, \tilde{\mathcal{R}}_K, \tilde{\mathcal{K}}_K, \tilde{\mathcal{R}}_K^*, \tilde{\mathcal{K}}_K^*\right]^T \tag{33}$$

with the $N \times 1$ matrix $\tilde{\mathcal{X}}_K$ and $N^2 \times 1$ matrices $\tilde{\mathcal{R}}_K$, $\tilde{\mathcal{K}}_K$ given in Appendix D (Eqs. (D.8)–(D.12)).

2.2. Time Domain Response

So far, all our results were given in the trap basis and hold for a general interatomic interaction potential. In the following numerical calculations, we approximate the interatomic potential $V(\mathbf{r} - \mathbf{r}')$ in Eq. (6) by a contact potential:

$$V(\mathbf{r} - \mathbf{r}') \longrightarrow U_0\delta(\mathbf{r} - \mathbf{r}'), \quad U_0 = \frac{4\pi\hbar^2 a}{m}, \tag{34}$$

where a is the s-wave scattering length and m is the atomic mass. This is valid because wave functions at ultracold temperatures have very long wavelengths compared to the range of interatomic potential implying that details of the interatomic potential become unimportant. The tetradic matrices V_{ijkl} defined in Eq. (6) are then simply given by

$$V_{ijkl} = \frac{4\pi\hbar^2 a}{m}\int \phi_i^*(\mathbf{r})\phi_j^*(\mathbf{r})\phi_k(\mathbf{r})\phi_l(\mathbf{r})d\mathbf{r}. \tag{35}$$

We consider a 2000-atom one-dimensional (1D) condensate in a harmonic trap. As demonstrated by the extensive body of literature so far, consideration of a 1D BEC helps us to identify key features of a BEC when full 3D simulation is computationally prohibitive. The parameters used for our numerical calculation of $\vec{\psi}^{(0)}$ are as follows: $U_0 = \frac{4\pi\hbar^2 a}{m} = 0.01$, and temperatures $0\hbar\omega_{\text{trap}}/k$ and $10\hbar\omega_{\text{trap}}/k$, where ω_{trap} is the trap frequency, k is the Boltzmann constant, and the basis set size of $N = 5$ is used, which was found to be sufficient for the purposes of simulation; a higher basis number did not noticeably alter the final results. We keep the trap units throughout with 256 grid points for position. The same parameters were used in the calculations of the linear response in [7].

To solve for the second-order response, both the zeroth- and the first-order solutions must be found. Calculation of the zeroth-order solution from the TIHFB equations is the most numerically involved step, as it requires solving nonlinear coupled equations. Griffin has provided a self-consistent prescription for solving the TIHFB, in terms of the Bogoliubov–de Gennes equations [10]. We have therefore followed the prescription of [10] to find the solution to TIHFB. Once the zeroth-order solution is found, it is straightforward to calculate the first- and the second-order response functions. The calculation of the eigenvalues of the non-Hermitian matrix $\mathcal{L}^{(2)}$ required for computing the response functions was carried out using the Arnoldi algorithm [36].

In order to provide an indication of the structure of the matrix $\mathcal{L}^{(2)}$, we first plot in Fig. 1 the linear susceptibility $K^{(1)}(\Omega, \mathbf{r} = 0, \mathbf{r}_1 = 0)$ for zero and finite temperatures. Peak positions indicate the resonant frequencies.

The second-order time domain response functions given in Eqs. (18)–(20) and Appendix C have been calculated. We first obtained the numerical solution to TIHFB; the $2N(2N + 1) \times 1$ vector $\vec{\psi}^{(0)}$ evaluated at zero and finite temperatures; the $2N(2N + 1) \times 2N(2N + 1)$ matrices $\tilde{\Upsilon}$, $\mathcal{U}$, and $\tilde{\Phi}$ defined in Eqs. (15), (23), and (24); and the $2N(2N + 1) \times 1$ vector $\vec{\Xi}_K$ defined in Eqs. (25) and (C.8). Substituting these into Eqs. (21) and (22), the final calculation involves matrix multiplication of $2N(2N + 1) \times 1$ vectors $\vec{\psi}^{(0)}$ and $\vec{\Xi}_K$ with $2N(2N + 1) \times 2N(2N + 1)$ matrices $\tilde{\Upsilon}$, $\mathcal{U}$, and $\tilde{\Phi}$ and integration over the time variable τ. $\tilde{\Upsilon}$ and $\tilde{\Phi}$ are constructed in terms of the harmonic oscillator basis states, which are calculated numerically from the recursive formula that involves the Gaussian function multiplying the Hermite polynomials [37]. The matrix $\mathcal{U}$ is calculated using a MATLAB function that uses the Padé approximation for matrix exponentiation [38].

We present the second-order response function in the time domain $K^{(2)}(t, t_1, t_2, \mathbf{r}, \mathbf{r}_1, \mathbf{r}_2)$ as a function of $\mathbf{r}$ and $\mathbf{r}_1$ at various times t, t_1, t_2 and $\mathbf{r}_2$. This provides a way to depict graphically the correlation involving six variables t, t_1, t_2, $\mathbf{r}$, $\mathbf{r}_1$, and $\mathbf{r}_2$ on a two-dimensional plot and gives a "snapshot" of the position-dependent second-order correlations across the condensate. The times t, t_1, and t_2 are, respectively, the time of detection and the time of the first and second applied short fields, while $\mathbf{r}$, $\mathbf{r}_1$, and $\mathbf{r}_2$ denote the corresponding spatial variables. The position dependence is important since the experimentally produced condensates are mesoscopic in size; in optical spectroscopy, however, the dipole approximation usually applies and, consequently, the spatial dependence of the response is irrelevant. Figure 2 shows the absolute value of the second-order response functions in the time domain with the time t_2 fixed at $t_2 = 0$. Figure 2a is for the position of perturbation fixed

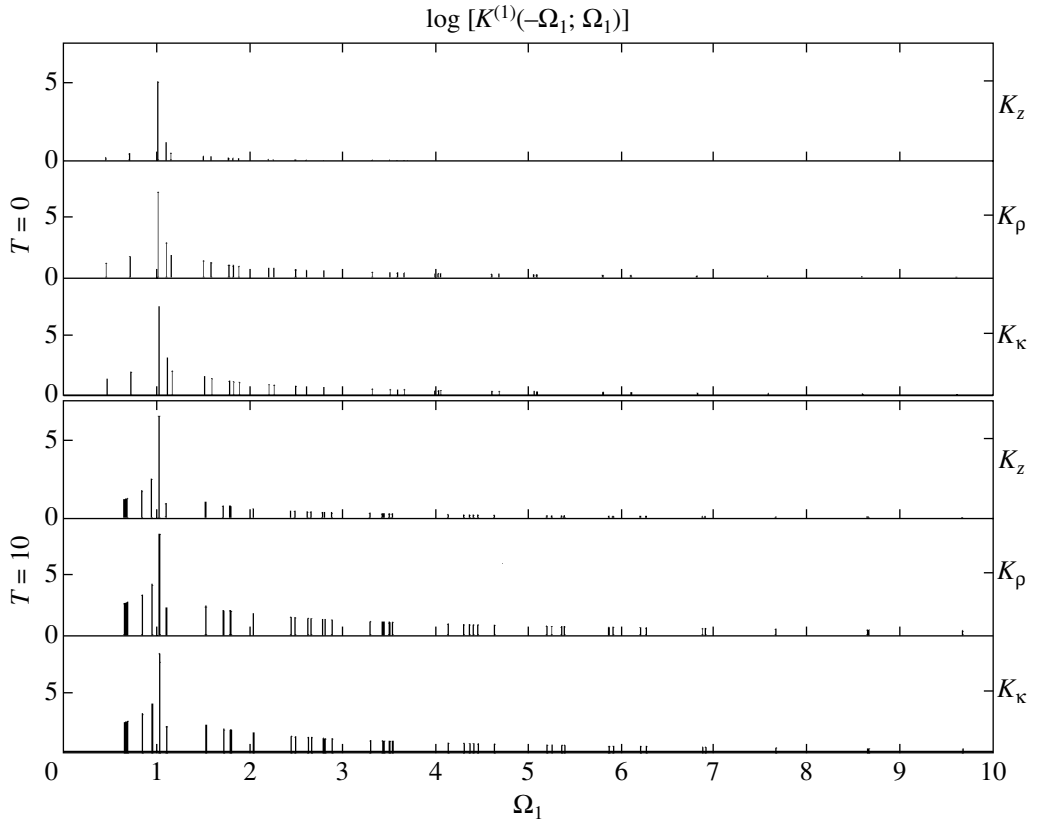

Fig. 1. Natural log of linear susceptibility $K^{(1)}(\Omega, \mathbf{r}, \mathbf{r}_1)$ at $\mathbf{r} = \mathbf{r}_1 = 0$ vs. frequency. Top three panels, zero temperature; bottom three panels, finite temperature $10\hbar\omega/k$. The frequency Ω_1 is given in units of the trap frequency.

at $\mathbf{r}_2 = 0$, i.e., the center of the trapped atomic cloud, while Fig. 2b is for $\mathbf{r}_2 = -5$ at the edge of the cloud. All positions are referred to in harmonic oscillator length units. The plots are for zero-temperature condensate at the short, intermediate, and long times ($\{t, t_1\} = \{5.89, 2.6\}$, $\{t, t_1\} = \{15.7, 7.2\}$, $\{t, t_1\} = \{31.4, 15.7\}$) as indicated at the top of each column of the figures. The times are given in units of the trap period, $1/\omega_{trap}$. The top, middle, and bottom rows give the response function for the condensate z, noncondensate density ρ, and noncondensate correlation κ, respectively. The dashed circle represents the spatial extent of the trapped BEC. The corresponding plot for a finite-temperature BEC at temperature $T = 10\hbar\omega_{trap}/k$ is displayed in Fig. 3.

The spatially asymmetric function at $\mathbf{r}_2 = -5$ reverse shape for $\mathbf{r}_2 = 5$, with similar changes also observed for the $\mathbf{r}_2 = \pm 2.5$ pair. With $\mathbf{r}_2 = \pm 2.5$, which is a point inside the atomic cloud, the contours had a markedly less symmetric shape than for $\mathbf{r}_2 = \pm 5$ at the very edge of the atomic cloud. The response functions take a more symmetric shape as time increases. The $\mathbf{r}_2$ dependence of the response function is found to be reduced at longer times. Comparing Figs. 2 and 3, the response functions clearly show a strong temperature dependence, with the functions giving distinct contours at different temperatures. The response functions attain spatial symmetry more rapidly at zero temperature owing to the weaker coupling between the variables z, ρ, and κ.

2.3. Frequency Domain Response

Using Eqs. (27)–(29), we have calculated the second-order susceptibility. It involves matrix multiplication of $2N(2N + 1) \times 1$ vectors $\vec{\psi}^{(0)}$ and $\vec{\Xi}_K(\omega)$ defined in Appendix D with the $2N(2N + 1) \times 2N(2N + 1)$ matrices $\tilde{\Upsilon}$, $\mathcal{U}(\omega)$, and $\tilde{\Phi}$. The Green's function $\mathcal{U}(\omega)$ is calculated as follows:

$$\mathcal{U}(\omega) = \frac{1}{\omega - \mathcal{L}^{(2)} + i\epsilon} = \sum_\nu \frac{\xi_\nu \zeta_\nu^\dagger}{\omega - \omega_\nu + i\epsilon}, \qquad (36)$$

where ξ_ν is the right eigenvector of $\mathcal{L}^{(2)}$ with eigenvalues ω_ν such that $\mathcal{L}^{(2)}\xi_\nu = \omega_\nu\xi_\nu$ and ζ_ν are the left eigenvectors of $\mathcal{L}^{(2)}$ such that $\sum_\nu \xi_\nu \zeta_\nu^\dagger = 1$. The eigenvalues ω_ν of $\mathcal{L}^{(2)}$ were calculated using the Arnoldi algorithm [36].

The absolute value of the second-order response function in the frequency domain $|K^{(2)}(\Omega, \Omega_1, \Omega_2, \mathbf{r}, \mathbf{r}_1, \mathbf{r}_2)|$ is

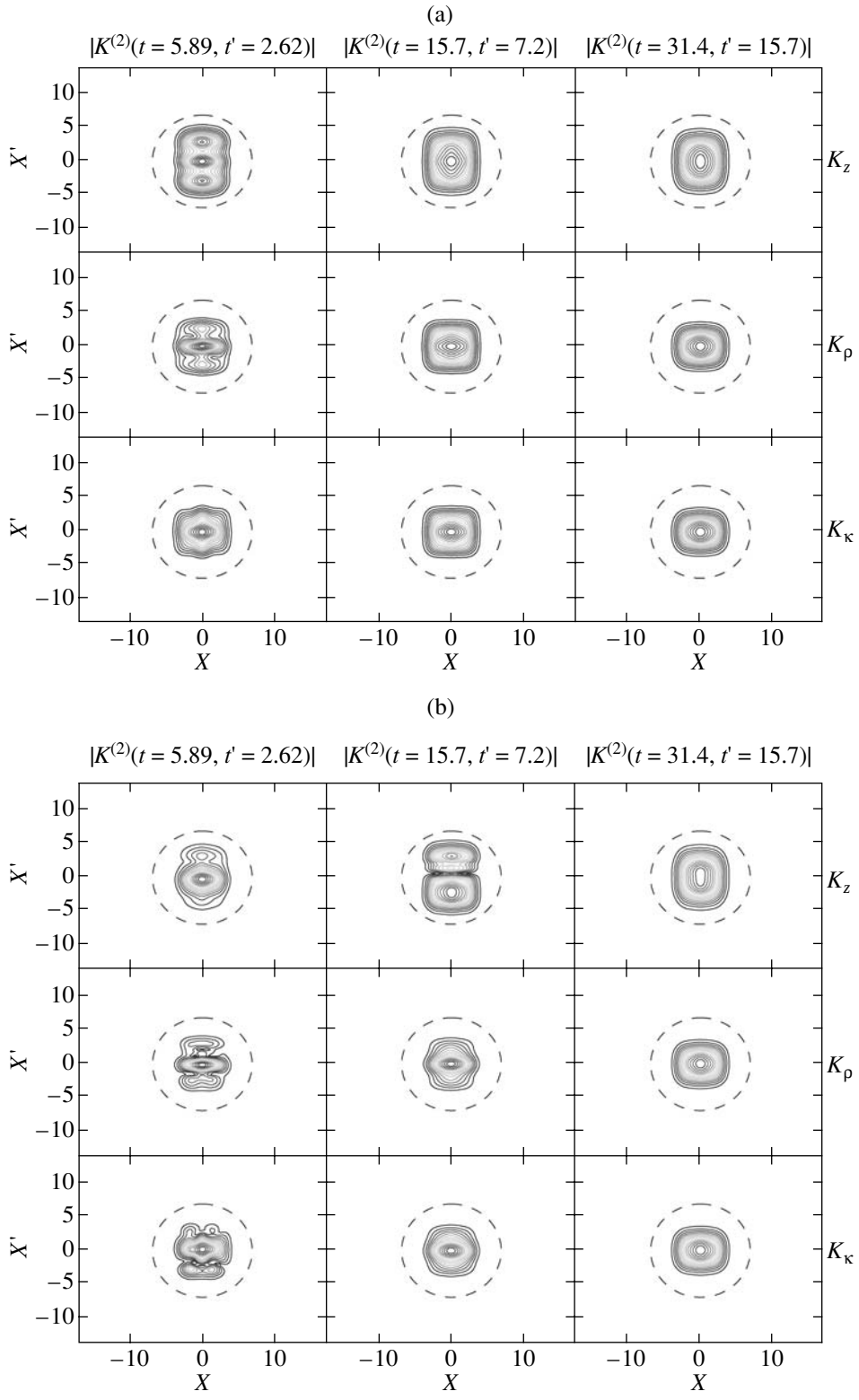

Fig. 2. $|K^{(2)}(t, t_1, t_2, \mathbf{r}, \mathbf{r}_1, \mathbf{r}_2)|$, i.e., the absolute value of the second-order response functions in the time domain with the time t_2 fixed at $t_2 = 0$. (a) $\mathbf{r}_2 = 0$; (b) $\mathbf{r}_2 = -5$. The plots are for zero-temperature condensate at the short, intermediate, and long times t and t_1 written at the top of each column of the figures. The top, middle, and bottom rows give the response function for the condensate, noncondensate density, and noncondensate correlation, respectively. The diameter of the dashed circle represents the spatial extent of the trapped BEC. The positions x and x' are given in harmonic oscillator length units.

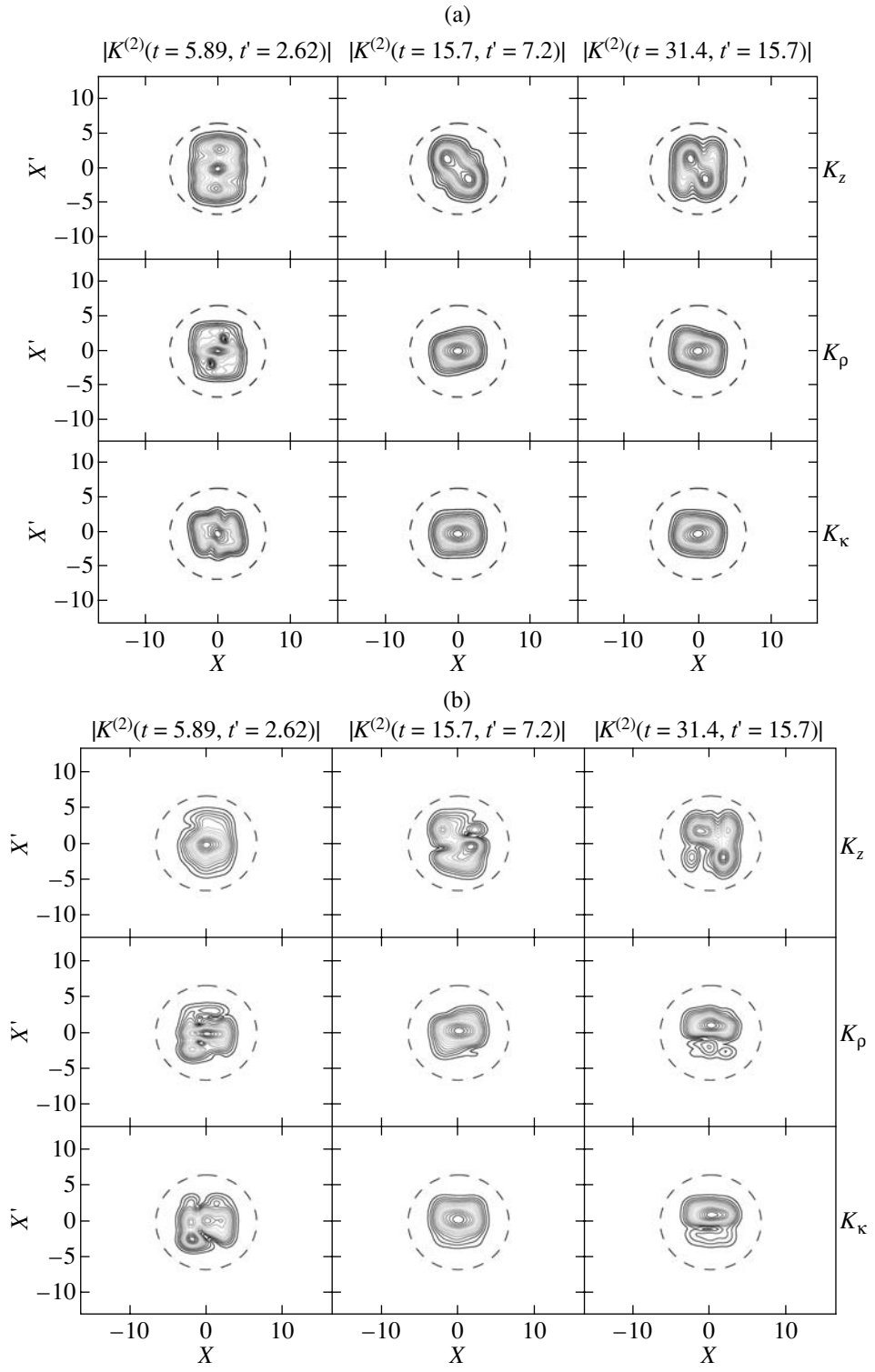

Fig. 3. The same as in Fig. 2, but at a finite temperature of $10\hbar\omega/k$. The positions x and x' are given in harmonic oscillator length units.

displayed in Fig. 4 with the position variable $\mathbf{r}_2$ set at (a) $\mathbf{r}_2 = 0$ at the center of the atomic cloud and (b) $\mathbf{r}_2 = -5$ at the edge of the atomic cloud. The plots are for zero-temperature condensate at various frequencies Ω_1 and Ω_2 indicated at the top of each column. We chose the frequencies such that Ω_1, Ω_2, and $\Omega_1 + \Omega_2$ are off-resonant with respect to the eigenvalues of $\mathcal{L}^{(2)}$ (first column, $\Omega_1 = 2.23$, $\Omega_2 = 1.55$); both Ω_1 and Ω_2 are on-

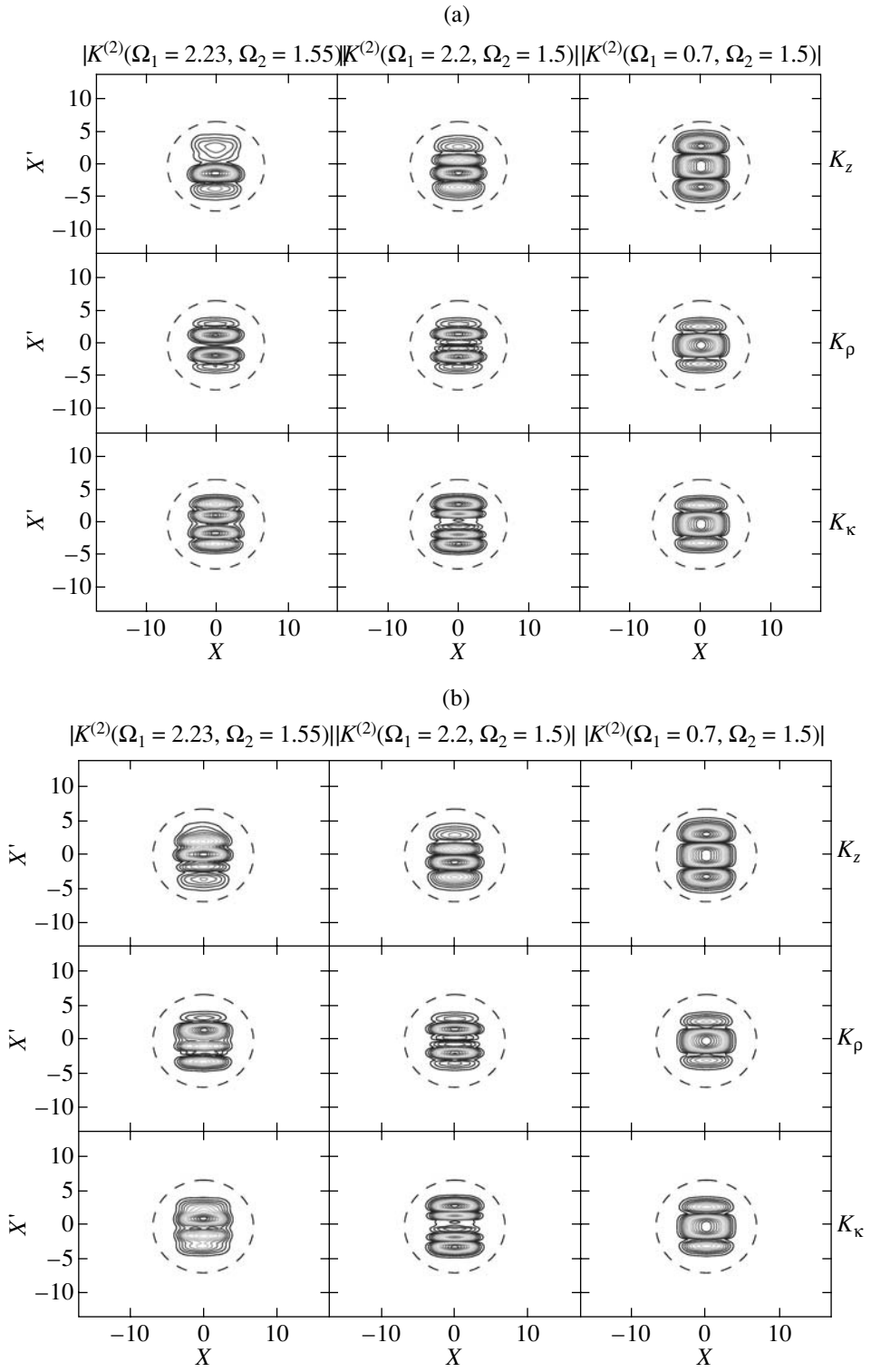

Fig. 4. $|K^{(2)}(\Omega, \Omega_1, \Omega_2, \mathbf{r}, \mathbf{r}_1, \mathbf{r}_2)|$, i.e., the absolute value of the second-order response functions in the frequency domain with the variable $\mathbf{r}_2$ set at (a) $\mathbf{r}_2 = 0$ and (b) $\mathbf{r}_2 = -5$. The plots are for zero-temperature condensate at the frequencies Ω_1 and Ω_2 given at the top of each column. Denoting "off-resonant" when the frequency does not match an eigenvalue of $\mathcal{L}^{(2)}$ and "on-resonance" when a frequency matches an eigenvalue, these frequencies are chosen such that Ω_1, Ω_2, and $\Omega_1 + \Omega_2$ are off-resonant ($\Omega_1 = 2.23$, $\Omega_2 = 1.55$); both Ω_1 and Ω_2 are on-resonance while $\Omega_1 + \Omega_2$ is off-resonant ($\Omega_1 = 2.2$, $\Omega_2 = 1.5$); and, finally, frequencies chosen so that $\Omega_1 + \Omega_2$ is on-resonance ($\Omega_1 = 0.7$, $\Omega_2 = 1.5$). The top, middle, and bottom rows give the response function for the condensate, noncondensate density, and noncondensate correlation, respectively. The diameter of the dashed circle represents the spatial extent of the trapped BEC. The positions x and x' are given in harmonic oscillator length units.

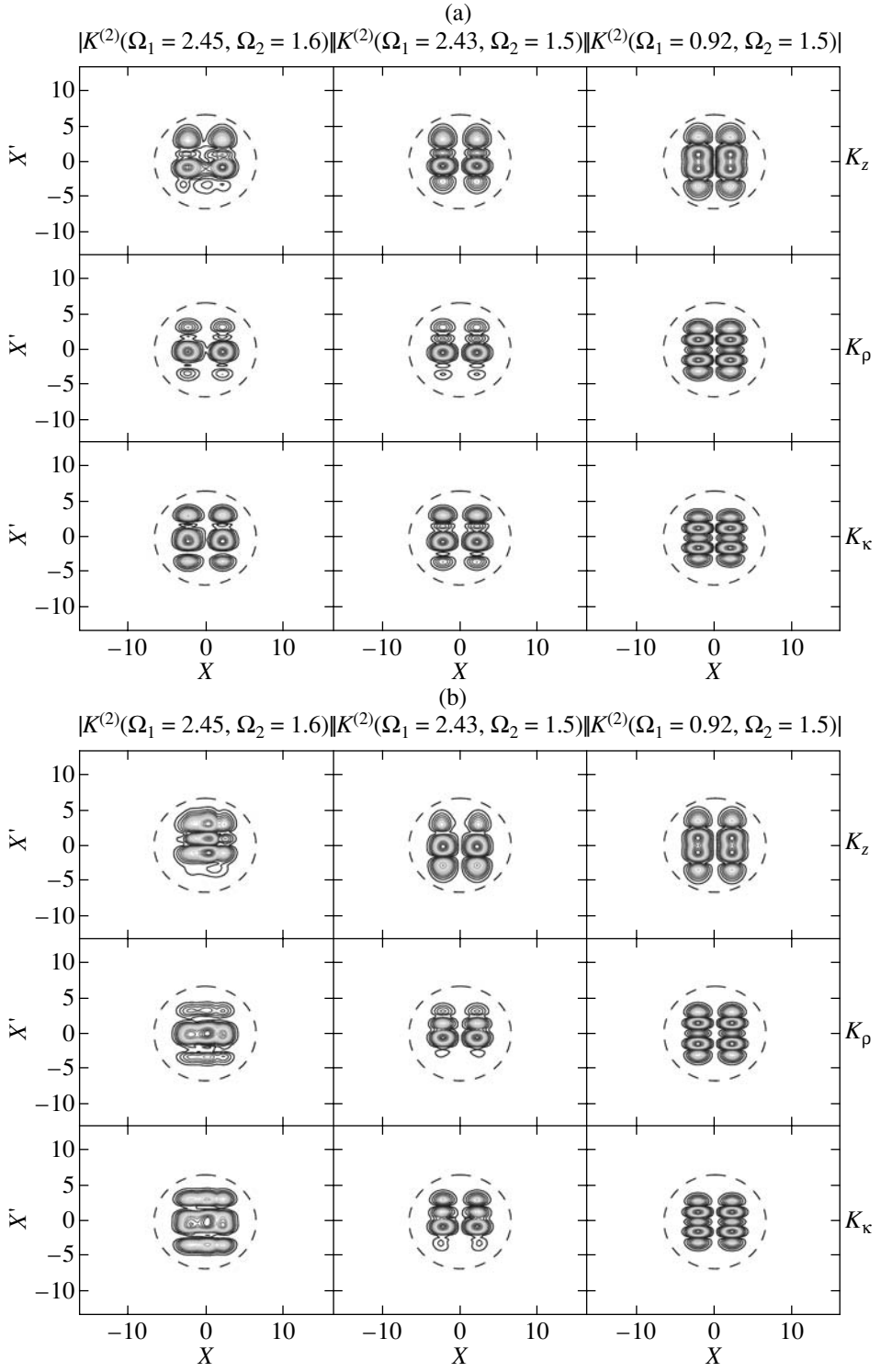

Fig. 5. The same as in Fig. 4, but at a finite temperature of $10\hbar\omega/k$. At finite temperature, the resonant frequencies are shifted from the zero-temperature counterpart, so that the actual frequency combinations used are the following: Ω_1, Ω_2, and $\Omega_1 + \Omega_2$ are off-resonant ($\Omega_1 = 2.45$, $\Omega_2 = 1.6$); both Ω_1 and Ω_2 are on-resonance with $\Omega_1 + \Omega_2$ off-resonant ($\Omega_1 = 2.43$, $\Omega_2 = 1.5$); and, finally, $\Omega_1 + \Omega_2$ is on-resonance ($\Omega_1 = 0.92$, $\Omega_2 = 1.5$). The positions x and x' are given in harmonic oscillator length units.

resonance, while $\Omega_1 + \Omega_2$ is off-resonant (second column, $\Omega_1 = 2.2$, $\Omega_2 = 1.5$); and, finally, $\Omega_1 + \Omega_2$ and Ω_2 are on-resonance ($\Omega_1 = 0.7$, $\Omega_2 = 1.5$). As with the previous figures, the top, middle, and bottom rows give the response function for the condensate, noncondensate density, and noncondensate correlation, respectively. The result for a finite-temperature BEC at temperature $T = 10\hbar\omega_{trap}/k$ is displayed in Fig. 5. At finite tempera-

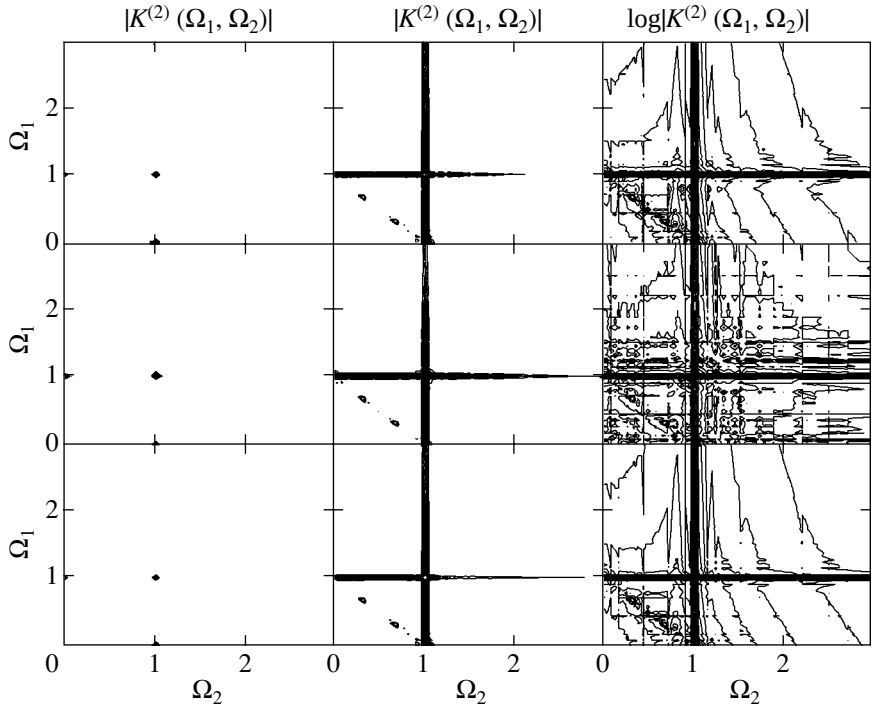

Fig. 6. (Left column) $|K^{(2)}(\Omega_1, \Omega_2)|$, i.e., the absolute value of the second-order response functions in the frequency domain as a function of Ω_1 and Ω_2 with the position variables set at $\mathbf{r} = \mathbf{r}_1 = \mathbf{r}_2 = 0$. There are three large peaks that completely dominate the plot, so the remaining peaks are not represented in the plot. (Center column) Scaled $|K^{(2)}(\Omega_1, \Omega_2)|$. The three largest peaks shown in the left column were scaled down to the same magnitude as other peaks in the plot. (Right column) $\log|K^{(2)}(\Omega_1, \Omega_2)|$, i.e., logarithm of the response functions presented in the left column to help visualize the large variation in the magnitude of $|K^{(2)}(\Omega_1, \Omega_2)|$. The top, middle, and bottom rows give the response function for the condensate, noncondensate density, and noncondensate correlation, respectively. The frequencies Ω_1 and Ω_2 are given in units of the trap frequency.

ture, the resonant frequencies are shifted from the zero-temperature counterpart, so that the actual frequency combinations used are the following: Ω_1, Ω_2, and $\Omega_1 + \Omega_2$ are off-resonant ($\Omega_1 = 2.45$, $\Omega_2 = 1.6$); both Ω_1 and Ω_2 are on-resonance, while $\Omega_1 + \Omega_2$ is off-resonant ($\Omega_1 = 2.43$, $\Omega_2 = 1.5$); and frequencies with $\Omega_1 + \Omega_2$ are on-resonance ($\Omega_1 = 0.92$, $\Omega_2 = 1.5$).

The susceptibilities become more spatially symmetric as resonant frequencies are matched. The most symmetric function was generated when the sum of two frequencies Ω_1 and Ω_2 was on-resonance, while the least symmetric function resulted when both frequencies were off-resonant. When only of one of the frequencies was on-resonance, a result with an intermediate level of symmetry was observed. The dependence of the response function on $\mathbf{r}_2$ is strongest for the off-resonant case, while the one where $\Omega_1 + \Omega_2$ is on-resonance remains more or less unaffected by the changes. As in the time domain response, the asymmetric function at $\mathbf{r}_2 = -5$ reverse shape for $\mathbf{r}_2 = 5$. Such change was also observed for the $\mathbf{r}_2 = \pm 2.5$ pair; again, for $\mathbf{r}_2 = \pm 2.5$, which is inside the atomic cloud, the contours were found to be less symmetric than the corresponding figures for $\mathbf{r}_2 = \pm 5$.

In Fig. 6, we plot the second-order susceptibility at zero temperature as a function of Ω_1 and Ω_2 with the position variables set at $\mathbf{r} = \mathbf{r}_1 = \mathbf{r}_2 = 0$, i.e., at the center of the atomic cloud. The left column shows $|K^{(2)}(\Omega_1, \Omega_2)|$, i.e., the absolute value of the second-order response function. The plot shows only few peaks near the frequency of 1 because the difference between the magnitude of these highest few peaks and the rest of the peaks occurring at other frequencies is too large. This suggests that one should ideally tune into the combination of frequencies Ω_1 and Ω_2 corresponding to these highest peaks to observe the maximum second-order response experimentally. The second frequency Ω_2 implies a completely different physics compared to the linear response; Ω_2 is the frequency of a new harmonic being generated as a result of a strong external perturbation oscillating at frequency Ω_1. The middle column of Fig. 6 gives $|K^{(2)}(\Omega_1, \Omega_2)|$, where the largest peaks are scaled down to the magnitude of the smaller peaks present. It clearly shows a number of peaks present at frequencies Ω_1 and Ω_2 less than 1 and also shows that, with Ω_1 (Ω_2) fixed at 1, there is a pronounced response for many values of Ω_2 (Ω_1). The right column of Fig. 6 shows the logarithm of the left column. This enables the

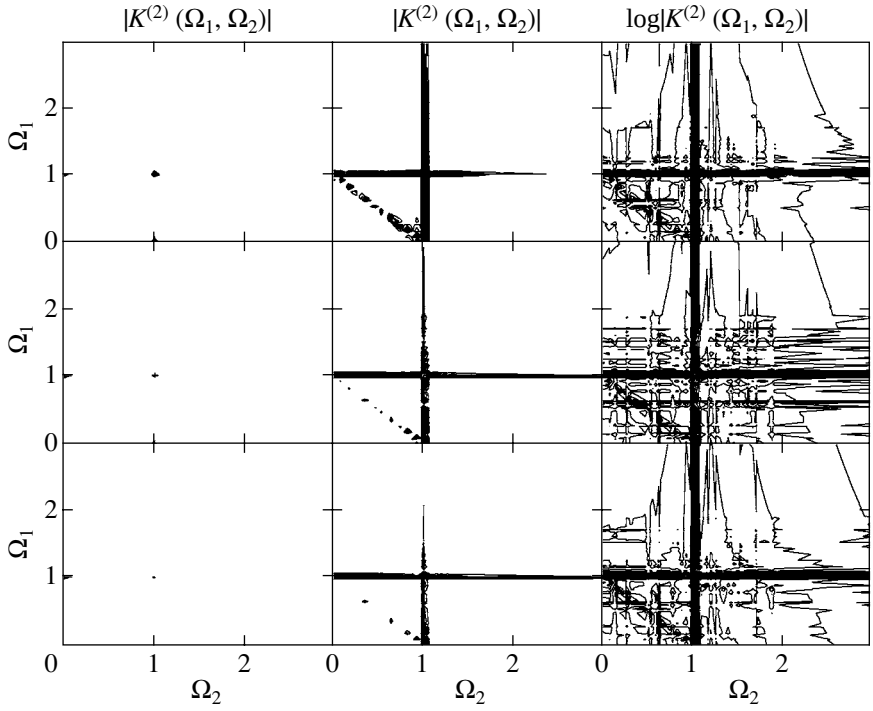

Fig. 7. The same as in Fig. 6, but at a finite temperature of $10\hbar\omega/k$. The frequencies Ω_1 and Ω_2 are given in units of the trap frequency.

large variations in the magnitude of $|K^{(2)}(\Omega_1, \Omega_2)|$ to be displayed. The top, middle, and bottom rows give the response function for the condensate, noncondensate density, and noncondensate correlation, respectively. Figure 7 shows the corresponding plot at the finite temperature $T = 10\hbar\omega_{\text{trap}}/k$. The main difference is that there are more peaks appearing around frequency $0 < \Omega_i < 1$, $i = 1, 2$ than at zero temperature.

Since the second-order susceptibility $K^{(2)}(\Omega_1, \Omega_2)$ is by itself a product of several Green's functions $\mathcal{U}(\omega)$ and linear susceptibilities $K^{(1)}(\omega)$, $\omega = \Omega_1$, Ω_2, and $\Omega_1 + \Omega_2$, several features of Figs. 6 and 7 are closely related to the linear susceptibility. From Fig. 1, it is clear that the linear susceptibility near the frequency of 1 dominates the spectrum at both zero and finite temperatures. It is therefore expected that any second-order response $K^{(2)}(\Omega_1, \Omega_2)$ containing a $\Omega_1 = 1$ or $\Omega_2 = 1$ component in it will lend a much stronger contribution to the spectrum than those not at $\Omega_1 = 1$ or $\Omega_2 = 1$. This explains the features around $\Omega_1 = 1$ and $\Omega_2 = 1$. In addition, the linear susceptibility $K^{(1)}(\omega)$ at finite temperature has more peaks around frequencies $0 < \omega < 1$ than at zero temperature, as there are more resonances below the frequency of 1 at finite temperature. This leads to the second-order susceptibility $K^{(2)}(\Omega_1, \Omega_2)$ displaying more peaks around frequency $0 < \Omega_1 < 1$ and $0 < \Omega_2 < 1$, as illustrated in Fig. 7.

3. NONLINEAR RESPONSE OF FRACTIONAL QUANTUM HALL SYSTEMS

In this section, we establish the correspondence between the FQHE effective Bose Hamiltonian and the Hamiltonian equations (1)–(6). With this correspondence, the nonlinear response functions derived above may be applied directly. We note that nonlinear response functions have not been extensively studied for FQHE systems, and, hence, this mapping provides a useful starting point. We start with the many-electron effective Hamiltonian $\hat{H}$, where the electron–electron interaction contains Coulomb repulsion $V(\mathbf{r} - \mathbf{r}') = 1/|\mathbf{r} - \mathbf{r}'|$, an external magnetic vector potential $\mathbf{A}(\mathbf{r})$, and an external electrical scalar potential $V_f(\mathbf{r}, t)$ [7, 40]:

$$\begin{aligned}\hat{H} &= \int dt \int d\mathbf{r}\, \hat{\psi}_e^\dagger(\mathbf{r}, t) \\ &\times \left(\frac{(-i\nabla_{\mathbf{r}} - e(\mathbf{A}(\mathbf{r})))^2}{2m} - \mu \right) \hat{\psi}_e(\mathbf{r}, t) \\ &+ \frac{1}{2} \int dt \int d\mathbf{r} \int d\mathbf{r}'\, \hat{\psi}_e^\dagger(\mathbf{r}, t) \hat{\psi}_e^\dagger(\mathbf{r}', t) \\ &\times V(\mathbf{r} - \mathbf{r}') \hat{\psi}_e(\mathbf{r}', t) \hat{\psi}_e(\mathbf{r}, t) \\ &+ \int dt \int d\mathbf{r}\, \hat{\psi}_e^\dagger(\mathbf{r}, t) V_f(\mathbf{r}, t) \hat{\psi}_e(\mathbf{r}, t),\end{aligned} \tag{37}$$

where $\hat{\psi}_e^\dagger(\mathbf{r}, t)$ and $\hat{\psi}_e(\mathbf{r}, t)$ are Fermi creation and annihilation operators, m is the effective electron band mass, and μ is the chemical potential.

We next introduce a quasiparticle creation operator $\hat{\psi}^{\dagger}(\mathbf{r}, t)$, which is related to $\hat{\psi}_e^{\dagger}(\mathbf{r}, t)$ as [31]

$$\begin{aligned}&\hat{\psi}^{\dagger}(\mathbf{r}, t)\\ &\equiv \hat{\psi}_e^{\dagger}(\mathbf{r}, t)\exp[-i\nu^{-1}\int d\mathbf{r}'\arg(\mathbf{r}-\mathbf{r}')\hat{n}(\mathbf{r}', t)],\end{aligned} \tag{38}$$

where $\arg(\mathbf{r}-\mathbf{r}')$ is the angle between the vector $(\mathbf{r}-\mathbf{r}')$ and the direction of the Hall current (which is perpendicular to both the external magnetic field $\mathbf{B}=\nabla_{\mathbf{r}}\times\mathbf{A}(\mathbf{r})$ and the external electric field $\mathbf{E}=-\nabla_{\mathbf{r}}V_f(\mathbf{r}, t)$, which are perpendicular to each other); ν^{-1} is an odd integer; and $\hat{n}(\mathbf{r}, t)$ is the charge density operator, which is the same for the actual Fermi and artificial Bose system,

$$\hat{n}(\mathbf{r}, t)\equiv\hat{\psi}_e^{\dagger}(\mathbf{r}, t)\hat{\psi}_e(\mathbf{r}, t) = \hat{\psi}^{\dagger}(\mathbf{r}, t)\hat{\psi}(\mathbf{r}, t). \tag{39}$$

The operators $\hat{\psi}^{\dagger}(\mathbf{r}, t)$ and $\hat{\psi}(\mathbf{r}, t)$ satisfy Bose commutation relations [26, 27]

$$\begin{aligned}\hat{\psi}(\mathbf{r})\hat{\psi}^{\dagger}(\mathbf{r}')-\hat{\psi}^{\dagger}(\mathbf{r}')\hat{\psi}(\mathbf{r}) &= \delta(\mathbf{r}-\mathbf{r}');\\ \hat{\psi}(\mathbf{r})\hat{\psi}(\mathbf{r}')-\hat{\psi}(\mathbf{r}')\hat{\psi}(\mathbf{r}) &= 0;\\ \hat{\psi}^{\dagger}(\mathbf{r})\hat{\psi}^{\dagger}(\mathbf{r}')-\hat{\psi}^{\dagger}(\mathbf{r}')\hat{\psi}^{\dagger}(\mathbf{r}) &= 0.\end{aligned} \tag{40}$$

Using the Bose quasiparticle operators (Eq. (38)), the Hamiltonian equation (37) can be written in the form of a many-boson effective Hamiltonian $\hat{H}$ by adding the gauge Chern–Simons vector potential $\mathbf{a}(\mathbf{r})$ [26, 28]:

$$\begin{aligned}\hat{H} &= \int dt\int d\mathbf{r}\hat{\psi}^{\dagger}(\mathbf{r}, t)\\ &\times\left(\frac{(-i\nabla_{\mathbf{r}}-e(\mathbf{A}(\mathbf{r})+\mathbf{a}(\mathbf{r})))^2}{2m}-\mu\right)\hat{\psi}(\mathbf{r}, t)\\ &+\frac{1}{2}\int dt\int d\mathbf{r}\int d\mathbf{r}'\hat{\psi}^{\dagger}(\mathbf{r}, t)\hat{\psi}^{\dagger}(\mathbf{r}', t)\\ &\times V(\mathbf{r}-\mathbf{r}')\hat{\psi}(\mathbf{r}', t)\hat{\psi}(\mathbf{r}, t)\\ &+\int dt\int d\mathbf{r}\hat{\psi}^{\dagger}(\mathbf{r}, t)V_f(\mathbf{r}, t)\hat{\psi}(\mathbf{r}, t).\end{aligned} \tag{41}$$

In order for the static Hall conductivity of the boson Hamiltonian equation (41) in Hartree–Fock–Bogoliubov approximation [6] to coincide with the conductivity obtained by using Laughlin's ansatz for the many-electron wave function [29], the magnetic and gauge potentials in k space should satisfy [28]

$$A_{\alpha}(k)+a_{\alpha}(k) = \frac{2\pi}{e\nu}\epsilon^{\alpha\beta}\frac{ik_{\beta}}{k^2}(\hat{n}_k-n). \tag{42}$$

Here, $\epsilon^{\alpha\beta}$ is a unit antisymmetric tensor,

$$\epsilon^{\alpha\beta}\equiv\begin{pmatrix}0 & 1\\ -1 & 0\end{pmatrix}; \tag{43}$$

n is the mean 2D electron density, $n=(m\nu\omega_c)/(2\pi)$; and the Fourier components of the charge density operator $\hat{n}_k$ with momentum k are

$$\hat{n}_k = \sum_k \hat{a}_k^{\dagger}\hat{a}_k, \tag{44}$$

where $\hat{a}_k^{\dagger}$ and $\hat{a}_k$ are Fourier components of $\hat{\psi}^{\dagger}(\mathbf{r})$ and $\hat{\psi}(\mathbf{r})$. Using a basis set of single electron functions $\phi_i(\mathbf{r})$, the field operators may be expanded in the form

$$\begin{aligned}\hat{\psi}^{\dagger}(\mathbf{r}, t) &= \sum_i \phi_i^*(\mathbf{r})\hat{a}_i^{\dagger}(t),\\ \hat{\psi}(\mathbf{r}, t) &= \sum_i \phi_i(\mathbf{r})\hat{a}_i(t),\end{aligned} \tag{45}$$

where $a_i^{\dagger}$ and a_i are Bose operators.

We make the following GCS Hartree–Fock–Bogoliubov ansatz for the time-dependent many-boson wave function [6, 9]:

$$\begin{aligned}|\psi(t)\rangle &= \exp\Big(\int dt\int d\mathbf{r}\alpha(\mathbf{r}, t)\hat{\psi}^{\dagger}(\mathbf{r})\\ &+\int dt\int d\mathbf{r}d\mathbf{r}'\beta(\mathbf{r}, \mathbf{r}', t)\hat{\psi}^{\dagger}(\mathbf{r})\hat{\psi}^{\dagger}(\mathbf{r}')\Big)|\Omega_0\rangle\\ &= \exp\left(\sum_i \alpha_i(t)\hat{a}_i^{\dagger}+\sum_{ij}\beta_{ij}(t)\hat{a}_i^{\dagger}\hat{a}_j^{\dagger}\right)|\Omega_0\rangle,\end{aligned} \tag{46}$$

where $|\Omega_0\rangle$ is an arbitrary normalized reference state with $\langle\Omega_0|\Omega_0\rangle=1$ [6].

On the other hand, the operator set of GCS generators of the closed algebra [39, 40] in the exponent of the ansatz equation (46) creates an extended Heisenberg–Weyl algebra, which may be obtained by a repeated application of the standard boson commutators.

The Hamiltonian that describes the system of many-body interacting bosons is obtained and comes from the basis set expansion of the Hamiltonian equation (41) and is given by [28]

$$\begin{aligned}\hat{H} &= \sum_{ij}\hat{H}_{ij}\hat{a}_i^{\dagger}\hat{a}_j+\sum_{ijkl}V_{ijkl}\hat{a}_i^{\dagger}\hat{a}_j^{\dagger}\hat{a}_k\hat{a}_l\\ &+\eta\sum_{ij}E_{ij}(t)\hat{a}_i^{\dagger}\hat{a}_j.\end{aligned} \tag{47}$$

Note that the Hamiltonian equation (47) coincides with Eqs. (1)–(6) provided we replace in Eq. (2) H_{ij}^{sp} by H_{ij}. In Eq. (47), the single-electron matrix element H_{ij} is given by

$$\begin{aligned}&H_{ij}\\ &= \int d\mathbf{r}\phi_i^*(\mathbf{r})\left(\frac{(-i\nabla_{\mathbf{r}}-e(\mathbf{A}(\mathbf{r})+\mathbf{a}(\mathbf{r})))^2}{2m}-\mu\right)\phi_j(\mathbf{r}),\end{aligned} \tag{48}$$

V_{ijkl} is a Coulomb repulsion between two electrons (we put electron charge $e=1$)

$$V_{ijkl} = \int d\mathbf{r}_1 d\mathbf{r}_2\phi_i^*(\mathbf{r}_1)\phi_j^*(\mathbf{r}_2)\frac{1}{|\mathbf{r}_1-\mathbf{r}_2|}\phi_k(\mathbf{r}_1)\phi_l(\mathbf{r}_2), \tag{49}$$

and the external electrical field $E(t)$ field expanded in a basis set is

$$\sum_{ij} E_{ij}(t)\hat{a}_i^\dagger \hat{a}_j = \int d\mathbf{r}\phi_i^*(\mathbf{r})V_f(\mathbf{r}, t)\phi_j(\mathbf{r})\hat{a}_i^\dagger \hat{a}_j. \quad (50)$$

We can therefore apply the results obtained for the Hamiltonian equations (1)–(6) to the FQHE by simply replacing H_{ij}^{sp} in Eq. (2) by H_{ij} (Eq. (48)).

Since, in a homogeneous system, the momentum is conserved, we can use the plane wave basis, i.e., the eigenfunctions of momentum $\mathbf{p}$ ($\phi_\mathbf{p}(\mathbf{r}) = S^{-1/2}\exp(-i\mathbf{pr})$, where S is the 2D volume of a system) by replacing the indices i by the momentum $\mathbf{p}$.

The second-order response is given by Eqs. (D.24)–(D.27) in the plane wave basis, provided that for the Hamiltonian we use Eqs. (1) and (2) in the Liouvillian equation (B.6) with $V_{\text{trap}} = 0$ and replace the interparticle interaction V_{ijkl} by

$$V_{\mathbf{p}-\mathbf{p}'} = \frac{2\pi e^2}{\epsilon|\mathbf{p}-\mathbf{p}'|} + \frac{4\pi^2 n}{m\nu^2|\mathbf{p}-\mathbf{p}'|^2}, \quad (51)$$

where the first term in the right-hand side represents the 2D Fourier transform component of the Coulomb repulsion and the second term comes from substituting Eq. (42) into Eq. (47). With these substitutions, the FQHE boson Hamiltonian equation (47) reduces to the classical form of Eq. (19) [28] and is equivalent to the classical boson Hamiltonian (Eq. (40) in [6]). The double excitations are given by the eigenvalues of the Liouvillian equation (B.6). The anisotropy in the gauge term equation (42) in the Hamiltonian equation (47) gives a nonvanishing second-order response, shifting the double-excitation energies with respect to twice the single excitations, as is the case in isotropic systems.

4. CONCLUSIONS

We have calculated the second-order response functions and susceptibilities of both zero- and finite-temperature Bose–Einstein condensates (BECs). The systematic, perturbative solution of the TDHFB equations for trapped, atomic BEC enables us to analyze the dynamics of finite-temperature BEC. The responses of both the noncondensate atoms and the condensate were calculated. The calculations apply for a general perturbation of the form $\sum_{ij}\int d^3\mathbf{r}\phi_i^*(\mathbf{r})V_f(\mathbf{r}, t)\hat{a}_i^\dagger \hat{a}_j$, where the shape of the external force $V_f(\mathbf{r}, t)$ is left arbitrary. The calculated second-order response functions were found to show a strong dependence on position and temperature. In the frequency domain, we have observed a distinct nonlinear mixing effect, which displays enhanced response at a number of Ω_1–Ω_2 combinations. The second-order response for BEC has not been reported yet, and most related recent work is limited to the linear response. As in optics, the second- and higher order response functions and susceptibilities are expected to be indispensable in characterizing the BEC dynamics in the presence of strong perturbations and, more importantly, in further development of matter-wave nonlinear optics [5].

We have also found that the second-order response functions calculated for an externally driven BEC are directly applicable to the important physical phenomenon of FQHE, and the GCS ansatz was applied for the derivation of the second-order response of FQHE in a 2D electron liquid. Although the relationship between a rapidly rotating BEC and QHE has been investigated previously [41], our results correspond to a case in which BEC is not necessarily rotating, providing a potentially useful conceptual connection between BEC and FQHE.

ACKNOWLEDGMENTS

The support of NSF (grant no. CHE-0132571) is gratefully acknowledged.

APPENDIX A

TDHFB EQUATIONS

The TDHFB equations of motion that couples z, ρ, and κ are [7, 11]

$$i\hbar\frac{dz}{dt} = [\mathcal{H}_z + \eta E(t)]z + \mathcal{H}_{z*}z^*, \quad (A.1)$$

$$i\hbar\frac{d\rho}{dt} = [h, \rho] - (\kappa\Delta^* - \Delta\kappa^*) + \eta[E(t), \rho], \quad (A.2)$$

$$i\hbar\frac{d\kappa}{dt} = (h\kappa + \kappa h^*) - (\rho\Delta - \Delta\rho^*) + \Delta + \eta[E(t), \kappa]_+, \quad (A.3)$$

where $[\ldots]_+$ denotes the anticommutator. Here, $\mathcal{H}_z$, $\mathcal{H}_{z*}$, h, and Δ are $N \times N$ matrices, with n being the number of basis wave functions used:

$$[\mathcal{H}_z]_{i,j} = H_{ij} - \mu + \sum_{kl} V_{iklj}[z_k^* z_l + 2\rho_{lk}], \quad (A.4)$$

$$[\mathcal{H}_{z*}]_{i,j} = \sum_{kl} V_{ijkl}\kappa_{kl}, \quad (A.5)$$

$$h_{ij} = H_{ij} - \mu + 2\sum_{kl} V_{iklj}[z_k^* z_l + \rho_{lk}], \quad (A.6)$$

$$\Delta_{ij} = \sum_{kl} V_{ijkl}[z_k z_l + \kappa_{kl}]. \quad (A.7)$$

h is known as the "Hartree–Fock Hamiltonian," and Δ as the "pairing field" [9]. μ is the chemical potential introduced in the Hamiltonian (Eq. (2)).

APPENDIX B

MATRIX $\mathcal{L}$ AND VECTOR ζ

In this appendix, we define the $2N(2N+1) \times 2N(2N+1)$ Liouvillian matrix of Eq. (7). As discussed in the main text, it suffices to define the zeroth- and the first-order matrices $\mathcal{L}^{(0)}$ and $\mathcal{L}^{(1)}$ only, since $\mathcal{L}^{(n)}$ for all $n \geq 1$ is identical. First of all, $\mathcal{L}^{(0)}$ is defined as follows:

$$\mathcal{L}^{(0)} = \begin{pmatrix} \mathcal{H}_z^{(0)} - \mu & \mathcal{H}_{z*}^{(0)} & 0 & 0 & 0 & 0 \\ \mathcal{H}_{z*}^{(0)*} & \mathcal{H}_z^{(0)*} - \mu & 0 & 0 & 0 & 0 \\ 0 & 0 & \mathcal{H}^{(-)} & \mathcal{D}^{\Delta} & 0 & \mathcal{D} \\ 0 & 0 & -\mathcal{D}^{\Delta *} & \mathcal{H}^{(+)} & \mathcal{D} & 0 \\ 0 & 0 & 0 & \mathcal{D}^{*} & \mathcal{H}^{(-)*} & \mathcal{D}^{\Delta *} \\ 0 & 0 & \mathcal{D}^{*} & 0 & -\mathcal{D}^{\Delta} & \mathcal{H}^{(+)*} \end{pmatrix}, \quad \text{(B.1)}$$

where $\mathcal{H}_z$ and $\mathcal{H}_{z*}$ of $\mathcal{L}^{(0)}$ are as defined in Eqs. (A.4) and (A.5) and the remaining $N^2 \times N^2$ submatrices are defined as

$$\mathcal{H}^{(-)}_{ij,mn} = h^{(0)}_{im}\delta_{jn} - h^{(0)}_{nj}\delta_{im}, \quad \text{(B.2)}$$

$$\mathcal{H}^{(+)}_{ij,mn} = h^{(0)}_{im}\delta_{jn} + h^{(0)}_{nj}\delta_{im} + V_{ijmn}, \quad \text{(B.3)}$$

$$\mathcal{D}_{ij,mn} = \Delta^{(0)}_{im}\delta_{jn}, \quad \text{(B.4)}$$

$$\mathcal{D}^{\Delta}_{ij,mn} = -\Delta^{*(0)}_{nj}\delta_{im}, \quad \text{(B.5)}$$

with $h^{(0)}$ and $\Delta^{(0)}$ being the Hartree–Fock Hamiltonian and the pairing field defined in Eqs. (A.6) and (A.7).

For higher orders $n \geq 1$ (in particular, $n = 2$),

$$\mathcal{L}^{(n)} \equiv \mathcal{L}^{(0)} + \mathcal{L}', \quad \text{(B.6)}$$

where $\mathcal{L}^{(0)}$ is the zeroth-order matrix defined above and

$$\mathcal{L}' = \begin{pmatrix} \mathcal{V}^{zz1} & \mathcal{V}^{zz2} & \mathcal{V}^{z1} & \mathcal{V}^{z2} & 0 & 0 \\ \mathcal{V}^{zz2*} & \mathcal{V}^{zz1*} & 0 & 0 & \mathcal{V}^{z1*} & \mathcal{V}^{z2*} \\ \mathcal{V}^{\rho z1} & \mathcal{V}^{\rho z2} & \mathcal{W}^{\rho h} & \mathcal{W}^{\kappa\Delta} & 0 & \mathcal{W}^{\kappa\Delta\dagger} \\ \mathcal{V}^{\kappa z1} & \mathcal{V}^{\kappa z2} & \mathcal{W}^{\kappa h} & \mathcal{W}^{\rho\Delta} & \mathcal{W}^{\kappa h\dagger} & 0 \\ \mathcal{V}^{\rho z2*} & \mathcal{V}^{\rho z1*} & 0 & (\mathcal{W}^{\kappa\Delta\dagger})^{*} & (\mathcal{W}^{\rho h})^{*} & (\mathcal{W}^{\kappa\Delta})^{*} \\ \mathcal{V}^{\kappa z2*} & \mathcal{V}^{\kappa z1*} & (\mathcal{W}^{\kappa h\dagger})^{*} & 0 & (\mathcal{W}^{\kappa h})^{*} & (\mathcal{W}^{\rho\Delta})^{*} \end{pmatrix}. \quad \text{(B.7)}$$

The set of $N \times N$ submatrices $\mathcal{V}^{zz1}$ and $\mathcal{V}^{zz2}$; $N \times N^2$ submatrices $\mathcal{V}^{z1}$ and $\mathcal{V}^{z2}$; $N^2 \times N$ submatrices $\mathcal{V}^{\rho z1}$, $\mathcal{V}^{\rho z2}$, $\mathcal{V}^{\kappa z1}$, and $\mathcal{V}^{\kappa z2}$; and $N^2 \times N^2$ component submatrices $\mathcal{W}^{\rho h}$, $\mathcal{W}^{\rho\Delta}$, $\mathcal{W}^{\kappa h}$, and $\mathcal{W}^{\kappa\Delta}$ of $\mathcal{L}'$ are given as follows:

$$\mathcal{V}^{zz1}_{i,l} = \sum_{kr} V_{iklr} z^{*(0)}_k z^{(0)}_r, \quad \mathcal{V}^{zz2}_{i,k} = \sum_{lr} V_{iklr} z^{(0)}_l z^{(0)}_r, \quad \text{(B.8)}$$

$$\mathcal{V}^{z1}_{i,kl} = 2\sum_{r} V_{ilkr} z^{(0)}_r, \quad \mathcal{V}^{z2}_{i,kl} = \sum_{r} V_{iklr} z^{(0)}_r, \quad \text{(B.9)}$$

$$\mathcal{V}^{\rho z1}_{ij,l} = 2\sum_{kr} V_{iklr} z^{*(0)}_k \rho^{(0)}_{rj} - V_{rklj} z^{*(0)}_k \rho^{(0)}_{ir} + \sum_{kr} [V_{irkl} z^{(0)}_k + V_{irlk} z^{(0)}_k] \kappa^{*(0)}_{rj}, \quad \text{(B.10)}$$

$$\mathcal{V}^{\rho z2}_{ij,k} = 2\sum_{lr} V_{iklr} z^{(0)}_l \rho^{(0)}_{rj} - V_{rklj} z^{(0)}_l \rho^{(0)}_{ir} - \sum_{lr} [V_{rjkl} z^{*(0)}_l + V_{rjlk} z^{*(0)}_l] \kappa^{(0)}_{ir}, \quad \text{(B.11)}$$

$$\mathcal{V}^{\kappa z1}_{ij,k} = 2\sum_{lr} V_{ilkr} z^{*(0)}_l \kappa^{(0)}_{rj} + V_{rklj} z^{*(0)}_l \kappa^{(0)}_{ir} + \sum_{kr} [V_{rjkl} z^{(0)}_l + V_{rjlk} z^{(0)}_l] \rho^{(0)}_{ir} + \sum_{lr} [V_{irkl} z^{(0)}_l + V_{irlk} z^{(0)}_l] \rho^{*(0)}_{rj} + \sum_{l} [V_{ijkl} z^{(0)}_l + V_{ijlk} z^{(0)}_l], \quad \text{(B.12)}$$

$$\mathcal{V}^{\kappa z2}_{ij,k} = 2\sum_{lr} V_{iklr} z^{(0)}_l \kappa^{(0)}_{rj} + V_{rlkj} z^{(0)}_l \kappa^{(0)}_{ir}, \quad \text{(B.13)}$$

$$\begin{aligned} \mathcal{W}^{\rho h}_{ij,kl} &= 2\sum_r V_{iklr}\rho^{(0)}_{rj} - V_{rklj}\rho^{(0)}_{ir}, \\ \mathcal{W}^{\rho\Delta}_{ij,kl} &= \sum_r V_{irkl}\rho^{(0)*}_{rj} + V_{rjkl}\rho^{(0)}_{ir}, \end{aligned} \quad \text{(B.14)}$$

$$\mathcal{W}^{\kappa h}_{ij,kl} = \sum_r V_{iklr}\kappa^{(0)}_{rj}, \quad \mathcal{W}^{\kappa h\dagger}_{ij,kl} = \sum_r V_{rklj}\kappa^{(0)}_{ir}, \quad \text{(B.15)}$$

$$\mathcal{W}^{\kappa\Delta}_{ij,kl} = \sum_r V_{irkl}\kappa^{(0)*}_{rj}, \quad \mathcal{W}^{\kappa\Delta\dagger}_{ij,kl} = \sum_r V_{rjkl}\kappa^{(0)}_{ir}. \quad \text{(B.16)}$$

In addition, the $2N(2N+1)\times 1$ vector $\zeta(t)$ is defined as follows:

$$\zeta(t) \equiv \begin{pmatrix} E(t) & 0 & 0 & 0 & 0 & 0 \\ 0 & E^*(t) & 0 & 0 & 0 & 0 \\ 0 & 0 & \epsilon^{(-)}(t) & 0 & 0 & 0 \\ 0 & 0 & 0 & \epsilon^{(+)}(t) & 0 & 0 \\ 0 & 0 & 0 & 0 & [\epsilon^{(-)}(t)]^* & 0 \\ 0 & 0 & 0 & 0 & 0 & [\epsilon^{(+)}(t)]^* \end{pmatrix} \begin{pmatrix} \vec{z}^{(0)} \\ \vec{z}^{(0)*} \\ \vec{\rho}^{(0)} \\ \vec{\kappa}^{(0)} \\ \vec{\rho}^{(0)*} \\ \vec{\kappa}^{(0)*} \end{pmatrix}, \quad \text{(B.17)}$$

where $E(t)$ is as defined in Eq. (4) and we further define the $N^2 \times N^2$ submatrices,

$$\epsilon^{(\pm)}(t)_{ij,kl} = E_{ik}(t)\delta_{jl} \pm E_{lj}(t)\delta_{ik}. \quad \text{(B.18)}$$

APPENDIX C

SECOND-ORDER RESPONSE FUNCTIONS

In this appendix, we first summarize the final result for the response functions in Section C.1 and then provide a more detailed derivation in Section C.2. In the last subsection (Section C.3) of this appendix, we also show an alternative form for the response functions written on the basis of the eigenvectors of the Liouvillian.

C.1. Final Expression

The second-order response functions for the condensate, the noncondensate density, and the correlation that we use in our numerical calculations are given by Eqs. (18)–(20) [reproduced here as Eqs. (C.1)–(C.3)] as follows:

$$\begin{aligned} &K^{(2)}_z(t, t_1, t_2, \mathbf{r}, \mathbf{r}_1, \mathbf{r}_2) \\ &= \sum_{i=1}^{N} [\tilde{\Upsilon}(\mathbf{r})(\vec{K}^{(2)}_I(t, t_1, t_2, \mathbf{r}_1, \mathbf{r}_2) + \vec{K}^{(2)}_{II}(t, t_1, t_2, \mathbf{r}_1, \mathbf{r}_2))]_i, \end{aligned} \quad \text{(C.1)}$$

$$\begin{aligned} &K^{(2)}_\rho(t, t_1, t_2, \mathbf{r}, \mathbf{r}_1, \mathbf{r}_2) \\ &= \sum_{i=2N+1}^{2N+N^2} [\tilde{\Upsilon}(\mathbf{r})(\vec{K}^{(2)}_I(t, t_1, t_2, \mathbf{r}_1, \mathbf{r}_2) \\ &\quad + \vec{K}^{(2)}_{II}(t, t_1, t_2, \mathbf{r}_1, \mathbf{r}_2))]_i, \end{aligned} \quad \text{(C.2)}$$

$$\begin{aligned} &K^{(2)}_\kappa(t, t_1, t_2, \mathbf{r}, \mathbf{r}_1, \mathbf{r}_2) \\ &= \sum_{i=2N+N^2+1}^{2N+2N^2} [\tilde{\Upsilon}(\mathbf{r})(\vec{K}^{(2)}_I(t, t_1, t_2, \mathbf{r}_1, \mathbf{r}_2) \\ &\quad + \vec{K}^{(2)}_{II}(t, t_1, t_2, \mathbf{r}_1, \mathbf{r}_2))]_i. \end{aligned} \quad \text{(C.3)}$$

Here, $2N(2N+1) \times 2N(2N+1)$ matrix $\tilde{\Upsilon}(\mathbf{r})$ was defined in Eq. (15) and the $2N(2N+1)\times 1$ vectors $\vec{K}^{(2)}_I$ and $\vec{K}^{(2)}_{II}$ are defined as follows:

$$\begin{aligned} &\vec{K}^{(2)}_I(t, t_1, t_2, \mathbf{r}_1, \mathbf{r}_2) \\ &= \mathcal{U}(t-t_1)\tilde{\Phi}(\mathbf{r}_1)\mathcal{U}(t_1-t_2)\tilde{\Phi}(\mathbf{r}_2)\vec{\psi}^{(0)}, \end{aligned} \quad \text{(C.4)}$$

$$\begin{aligned} &\vec{K}^{(2)}_{II}(t, t_1, t_2, \mathbf{r}_1, \mathbf{r}_2) \\ &= \int_0^t d\tau \mathcal{U}(t-\tau)\vec{\Xi}_K(\tau - t_1, \tau - t_2, \mathbf{r}_1, \mathbf{r}_2), \end{aligned} \quad \text{(C.5)}$$

where $\mathcal{U}(t-t')$ and $\tilde{\Phi}(\mathbf{r}')$ are given by Eqs. (23) and (24), respectively. The vector $\vec{\Xi}_K$ of Eq. (22) [Eq. (C.5)] is written $\vec{\Xi}_K = [\mathcal{L}_K, \mathcal{L}_K^*, \mathcal{R}_K, \mathcal{H}_K, \mathcal{R}_K^*, \mathcal{H}_K^*]^T$ with the $N\times 1$ matrix $\mathcal{L}_K$ and $N^2\times 1$ matrices $\mathcal{R}_K$, $\mathcal{H}_K$ given as follows:

$$
\begin{aligned}
&[\mathcal{L}_K]_i \\
&= \sum_{klr} V_{iklr}[[\vec{K}_z^{(1)*}(\tau-t_1,\mathbf{r}_1)]_k z_l^{(0)}[\vec{K}_z^{(1)}(\tau-t_2,\mathbf{r}_2)]_r \\
&\quad + [\vec{K}_z^{(1)*}(\tau-t_1,\mathbf{r}_1)]_k[\vec{K}_z^{(1)}(\tau-t_2,\mathbf{r}_2)]_l z_r^{(0)} \\
&\quad + z_k^{*(0)}[\vec{K}_z^{(1)}(\tau-t_1,\mathbf{r}_1)]_l[\vec{K}_z^{(1)}(\tau-t_2,\mathbf{r}_2)]_r \\
&\qquad + 2[\vec{K}_\rho^{(1)}(\tau-t_1,\mathbf{r}_1)]_{lk}[\vec{K}_z^{(1)}(\tau-t_2,\mathbf{r}_2)]_r \\
&\qquad + [\vec{K}_\kappa^{(1)}(\tau-t_1,\mathbf{r}_1)]_{kl}[\vec{K}_z^{(1)}(\tau-t_2,\mathbf{r}_2)]_r],
\end{aligned}
\tag{C.6}
$$

$$
\begin{aligned}
&[\mathcal{R}_K]_{ij} \\
&= 2\sum_{rkl} V_{iklr}[\vec{K}_\rho^{(1)}(\tau-t_1,\mathbf{r}_1)]_{rj}[\vec{K}_\rho^{(1)}(\tau-t_2,\mathbf{r}_2)]_{kl} \\
&\quad - V_{rklj}[\vec{K}_\rho^{(1)}(\tau-t_1,\mathbf{r}_1)]_{kl}[\vec{K}_\rho^{(1)}(\tau-t_2,\mathbf{r}_2)]_{ir} \\
&\quad + \sum_{rkl} V_{iklr}[\vec{K}_\kappa^{(1)}(\tau-t_1,\mathbf{r}_1)]_{kl}[\vec{K}_\kappa^{*(1)}(\tau-t_2,\mathbf{r}_2)]_{rj} \\
&\quad + V_{rjkl}[\vec{K}_\kappa^{*(1)}(\tau-t_1,\mathbf{r}_1)]_{kl}[\vec{K}_\kappa^{(1)}(\tau-t_2,\mathbf{r}_2)]_{ir} \\
&\quad + 2\sum_{rkl} V_{iklr}[\vec{K}_z^{*(1)}(\tau-t_1,\mathbf{r}_1)]_k[\vec{K}_z^{(1)}(\tau-t_2,\mathbf{r}_2)]_l \rho_{rj}^{(0)} \\
&\quad - V_{rklj}[\vec{K}_z^{*(1)}(\tau-t_1,\mathbf{r}_1)]_k[\vec{K}_z^{(1)}(\tau-t_2,\mathbf{r}_2)]_l \rho_{ir}^{(0)} \\
&\quad + 2\sum_{rkl} V_{iklr}[[\vec{K}_z^{*(1)}(\tau-t_1,\mathbf{r}_1)]_k z_l^{(0)} \\
&\quad + z_k^{*(0)}[\vec{K}_z^{(1)}(\tau-t_1,\mathbf{r}_1)]_l][\vec{K}_\rho^{(1)}(\tau-t_2,\mathbf{r}_2)]_{rj} \\
&\quad - V_{rklj}[[\vec{K}_z^{*(1)}(\tau-t_1,\mathbf{r}_1)]_k z_l^{(0)} + z_k^{*(0)}[\vec{K}_z^{(1)}(\tau-t_1,\mathbf{r}_1)]_l] \\
&\quad \times [\vec{K}_\rho^{(1)}(\tau-t_2,\mathbf{r}_2)]_{ir} + \sum_{rkl} V_{rjkl}[[\vec{K}_z^{(1)*}(\tau-t_1,\mathbf{r}_1)]_k z_l^{*(0)} \\
&\quad + z_k^{*(0)}[\vec{K}_z^{*(1)}(\tau-t_1,\mathbf{r}_1)]_l][\vec{K}_\kappa^{(1)}(\tau-t_2,\mathbf{r}_2)]_{ir} \\
&\quad - V_{irkl}[[\vec{K}_z^{(1)}(\tau-t_1,\mathbf{r}_1)]_k z_l^{(0)} + z_k^{(0)}[\vec{K}_z^{(1)}(\tau-t_1,\mathbf{r}_1)]_l] \\
&\quad \times [\vec{K}_\kappa^{*(1)}(\tau-t_2,\mathbf{r}_2)]_{rj} + \sum_{rkl} V_{rjkl}[\vec{K}_z^{(1)}(\tau-t_1,\mathbf{r}_1)]_k \\
&\quad \times [\vec{K}_z^{(1)}(\tau-t_2,\mathbf{r}_2)]_k \kappa_{ir}^{(0)} \\
&\quad - V_{irkl}[\vec{K}_z^{(1)}(\tau-t_1,\mathbf{r}_1)]_k[\vec{K}_z^{(1)}(\tau-t_2,\mathbf{r}_2)]_l \kappa_{rj}^{*(0)},
\end{aligned}
\tag{C.7}
$$

$$
\begin{aligned}
&[\mathcal{H}_K]_{ij} \\
&= 2\sum_{rkl} V_{iklr}[\vec{K}_\kappa^{(1)}(\tau-t_1,\mathbf{r}_1)]_{rj}[\vec{K}_\rho^{(1)}(\tau-t_2,\mathbf{r}_2)]_{lk} \\
&\quad + V_{rklj}[\vec{K}_\rho^{(1)}(\tau-t_1,\mathbf{r}_1)]_{kl}[\vec{K}_\kappa^{(1)}(\tau-t_2,\mathbf{r}_2)]_{ir} \\
&\quad + \sum_{rkl} V_{irkl}[\vec{K}_\kappa^{(1)}(\tau-t_1,\mathbf{r}_1)]_{kl}[\vec{K}_\rho^{(1)*}(\tau-t_2,\mathbf{r}_2)]_{rj} \\
&\quad + V_{rjkl}[\vec{K}_\kappa^{(1)}(\tau-t_1,\mathbf{r}_1)]_{kl}[\vec{K}_\rho^{(1)}(\tau-t_2,\mathbf{r}_2)]_{ir} \\
&\quad + 2\sum_{rkl} V_{iklr}[\vec{K}_z^{*(1)}(\tau-t_1,\mathbf{r}_1)]_k[\vec{K}_z^{(1)}(\tau-t_2,\mathbf{r}_2)]_l \kappa_{rj}^{(0)} \\
&\quad + V_{rklj}[\vec{K}_z^{(1)}(\tau-t_1,\mathbf{r}_1)]_k[\vec{K}_z^{*(1)}(\tau-t_2,\mathbf{r}_2)]_l \kappa_{ir}^{(0)} \\
&\quad + 2\sum_{rkl} V_{iklr}[[\vec{K}_z^{*(1)}(\tau-t_1,\mathbf{r}_1)]_k z_l^{(0)} \\
&\quad + z_k^{*(0)}[\vec{K}_z^{(1)}(\tau-t_1,\mathbf{r}_1)]_l][\vec{K}_\kappa^{(2)}(\tau-t_1,\mathbf{r}_2)]_{rj} \\
&\quad + V_{rklj}[[\vec{K}_z^{(1)}(\tau-t_1,\mathbf{r}_1)]_k z_l^{*(0)} \\
&\quad + z_k^{(0)}[\vec{K}_z^{*(1)}(\tau-t_1,\mathbf{r}_1)]_l][\vec{K}_\kappa^{(1)}(\tau-t_2,\mathbf{r}_2)]_{ir} \\
&\quad + \sum_{rkl} V_{rjkl}[[\vec{K}_z^{(1)}(\tau-t_1,\mathbf{r}_1)]_k z_l^{(0)} \\
&\quad + z_k^{(0)}[\vec{K}_z^{(1)}(\tau-t_1,\mathbf{r}_1)]_l][\vec{K}_\rho^{(1)}(\tau-t_2,\mathbf{r}_2)]_{ir} \\
&\quad + V_{irkl}[[\vec{K}_z^{(1)}(\tau-t_1,\mathbf{r}_1)]_k z_l^{(0)} \\
&\quad + z_k^{(0)}[\vec{K}_z^{(1)}(\tau-t_1,\mathbf{r}_1)]_l][\vec{K}_\rho^{*(1)}(\tau-t_2,\mathbf{r}_2)]_{rj} \\
&\quad + \sum_{rkl} V_{rjkl}[\vec{K}_z^{(1)}(\tau-t_1,\mathbf{r}_1)]_k[\vec{K}_z^{(1)}(\tau-t_2,\mathbf{r}_2)]_l \rho_{ir}^{(0)} \\
&\quad + V_{irkl}[\vec{K}_z^{(1)}(\tau-t_1,\mathbf{r}_1)]_k[\vec{K}_z^{(1)}(\tau-t_2,\mathbf{r}_2)]_l \rho_{rj}^{*(0)} \\
&\quad + \sum_{kl} V_{ijkl}[\vec{K}_z^{(1)}(\tau-t_1,\mathbf{r}_1)]_k[\vec{K}_z^{(1)}(\tau-t_2,\mathbf{r}_2)]_l,
\end{aligned}
\tag{C.8}
$$

where the vectors $\vec{K}_z^{(1)}(\tau - t_i, \mathbf{r}_i)$, $\vec{K}_\rho^{(1)}(t - t_1, \mathbf{r}_i)$, and $\vec{K}_\kappa^{(1)}(\tau - t_i, \mathbf{r}_i)$ found in Eqs. (C.6)–(C.8) are defined as

$$\vec{K}_\alpha^{(1)}(\tau - t_i, \mathbf{r}_i) = \mathcal{U}^{(\alpha)}(\tau - t_i)\tilde{\Phi}(\mathbf{r}_i)\vec{\psi}^{(0)}, \quad \alpha = z, \rho, \kappa, \quad i = 1, 2. \tag{C.9}$$

$\mathcal{U}^{(\alpha)}(\tau - t_i)$ are the submatrices of $\mathcal{U}(t - t_1)$ such that

$$\mathcal{U}(t - t_1) = [\mathcal{U}^{(z)}(\tau - t_i), \mathcal{U}^{(z)*}(\tau - t_i), \mathcal{U}^{(\rho)}(\tau - t_i), \mathcal{U}^{(\kappa)}(\tau - t_i), \mathcal{U}^{(\rho)*}(\tau - t_i), \mathcal{U}^{(\kappa)*}(\tau - t_i)]^T, \tag{C.10}$$

where $\mathcal{U}^{(z)}(\tau - t_i)$ is an $N \times 2N(2N + 1)$ submatrix while $\mathcal{U}^{(\gamma)}(\tau - t_i)$, $\gamma = \rho, \kappa, \rho^*, \kappa^*$ is an $N^2 \times 2N(2N + 1)$ submatrix; i.e., the submatrix $\mathcal{U}^{(z)}(\tau - t_i)$ is stacked on top of submatrix $\mathcal{U}^{(z)*}(\tau - t_i)$, which, in turn, is stacked on top of submatrices $\mathcal{U}^{(\gamma)}(\tau - t_i)$. It is to be noted that $\vec{K}_\alpha^{(1)}(\tau - t_i, \mathbf{r}_i)$ as defined here are $N \times 1$ and $N^2 \times 1$ vectors, not scalar quantities obtained by integrating the scalar function $\vec{K}_\alpha^{(1)}(\tau - t_i, \mathbf{r}, \mathbf{r}_i)$ over $\mathbf{r}$.

C.2. Derivation

Writing the second-order solution to TDHFB explicitly, we have

$$\vec{\psi}^{(2)}(t) = \frac{1}{i\hbar}\int_0^t \exp\left[-\frac{i}{\hbar}\mathcal{L}^{(2)}(t - t_1)\right]\vec{\Gamma}(t_1)dt_1 \tag{C.11}$$

$$\equiv \frac{1}{i\hbar}\int_0^t \mathcal{U}(t - t_1)\vec{\Gamma}(t_1)dt_1. \tag{C.12}$$

Here,

$$\vec{\Gamma}(t_1) = \zeta(t_1)\vec{\psi}^{(1)}(t_1) + \vec{\Xi}(t_1), \tag{C.13}$$

i.e., for the second-order response, $\lambda^{(2)}(t) \equiv \zeta(t)\vec{\psi}^{(1)}(t) + \vec{\Xi}(t)$ in Eq. (7), where $\zeta(t)$ is given in Appendix B and $\vec{\Xi}(t)$ is a $2N(2N + 1) \times 1$ vector originating from the terms in the expansion that are made up of products of two first-order variables, i.e., $z^{(1)}$, $\rho^{(1)}$, and $\kappa^{(1)}$. The vector $\vec{\Xi}(t)$ can be written as $\vec{\Xi}(t) = [\mathcal{L}, \mathcal{L}^*, \mathcal{R}, \mathcal{H}, \mathcal{R}^*, \mathcal{H}^*]^T$ with the $N \times 1$ matrix $\mathcal{L}$, and $N^2 \times 1$ matrices $\mathcal{R}$, $\mathcal{H}$ given as follows:

$$\begin{aligned}\mathcal{L}_i = {} & \sum_{klr} V_{iklr}[z_k^{*(1)}z_l^{(0)}z_r^{(1)} + z_k^{*(1)}z_l^{(1)}z_r^{(0)} \\ & + z_k^{*(0)}z_l^{(1)}z_r^{(1)} + 2\rho_{lk}^{(001)}z_r^{(1)} + \kappa_{kl}^{(1)}z_r^{(1)}],\end{aligned} \tag{C.14}$$

$$\begin{aligned}\mathcal{R}_{ij} = {} & 2\sum_{rkl} V_{iklr}\rho_{rj}^{(1)}\rho_{kl}^{(1)} - V_{rklj}\rho_{kl}^{(1)}\rho_{ir}^{(1)} \\ & + \sum_{rkl} V_{irkl}\kappa_{kl}^{(1)}\kappa_{rj}^{*(1)} + V_{rjkl}\kappa_{kl}^{*(1)}\kappa_{ir}^{(1)} \\ & + 2\sum_{rkl} V_{iklr}z_k^{*(1)}z_l^{(1)}\rho_{rj}^{(0)} - V_{rklj}z_k^{*(1)}z_l^{(1)}\rho_{ir}^{(0)} \\ & + 2\sum_{rkl} V_{iklr}[z_k^{*(1)}z_l^{(0)} + z_k^{*(0)}z_l^{(1)}]\rho_{rj}^{(1)} \\ & - V_{rklj}[z_k^{*(1)}z_l^{(0)} + z_k^{*(0)}z_l^{(1)}]\rho_{ir}^{(1)} \\ & + \sum_{rkl} V_{rjkl}[z_k^{*(1)}z_l^{(0)} + z_k^{*(0)}z_l^{(1)}]\kappa_{ir}^{(1)} \\ & - V_{irkl}[z_k^{(1)}z_l^{(0)} + z_k^{(0)}z_l^{(1)}]\kappa_{rj}^{*(1)} \\ & + \sum_{rkl} V_{rjkl}z_k^{(1)}z_l^{(1)}\kappa_{ir}^{(0)} - V_{irkl}z_k^{(1)}z_l^{(1)}\kappa_{rj}^{(0)},\end{aligned} \tag{C.15}$$

$$\begin{aligned}\mathcal{H}_{ij} = {} & 2\sum_{rkl} V_{iklr}\kappa_{rj}^{(1)}\rho_{lk}^{(1)} + V_{rklj}\rho_{kl}^{(1)}\kappa_{ir}^{(1)} \\ & + \sum_{rkl} V_{irkl}\kappa_{kl}^{(1)}\rho_{rj}^{*(1)} + V_{rjkl}\kappa_{kl}^{(1)}\rho_{ir}^{(1)} \\ & + 2\sum_{rkl} V_{iklr}z_k^{*(1)}z_l^{(1)}\kappa_{rj}^{(0)} + V_{rklj}z_k^{(1)}z_l^{*(1)}\kappa_{ir}^{(0)} \\ & + 2\sum_{rkl} V_{iklr}[z_k^{*(1)}z_l^{(0)} + z_k^{*(0)}z_l^{(1)}]\kappa_{rj}^{(1)} \\ & + V_{rklj}[z_k^{(1)}z_l^{*(0)} + z_k^{(0)}z_l^{*(1)}]\kappa_{ir}^{(1)} \\ & + \sum_{rkl} V_{rjkl}[z_k^{(1)}z_l^{(0)} + z_k^{(0)}z_l^{(1)}]\rho_{ir}^{(1)} \\ & + V_{irkl}[z_k^{(1)}z_l^{(0)} + z_k^{(0)}z_l^{(1)}]\rho_{rj}^{*(1)} \\ & + \sum_{rkl} V_{rjkl}z_k^{(1)}z_l^{(1)}\rho_{ir}^{(0)} + V_{irkl}z_k^{(1)}z_l^{(1)}\rho_{rj}^{*(1)} \\ & + \sum_{kl} V_{ijkl}z_k^{(1)}z_l^{(1)}.\end{aligned} \tag{C.16}$$

Casting Eq. (C.12) in the form

$$\vec{\psi}^{(2)}(\mathbf{r}, t) = \int \vec{K}^{(2)}(t, t_1, t_2, \mathbf{r}, \mathbf{r}_1, \mathbf{r}_2) \times V_f(\mathbf{r}_1, t_1)V_f(\mathbf{r}_2, t_2)d^3\mathbf{r}_1 dt_1 d^3\mathbf{r}_2 dt_2 \tag{C.17}$$

involves rewriting $\vec{\Gamma}(t)$ of Eq. (C.13) in the position-dependent form:

$$\vec{\Gamma}(t_1) = \frac{1}{i\hbar}\int_0^{t_1} dt_2 \int d\mathbf{r}_1 d\mathbf{r}_2 [\tilde{\Phi}(\mathbf{r}_1)\vec{K}^{(1)}(t_1, t_2, \mathbf{r}_2)] \times V_f(\mathbf{r}_1, t_1) V_f(\mathbf{r}_2, t_2) \quad \text{(C.18)}$$

$$+ \int_0^{t_1}\int_0^{t_1} dt_2 dt_3 \int d\mathbf{r}_2 d\mathbf{r}_3 [\vec{\Xi}_K(t_1 - t_2, t_1 - t_3; \mathbf{r}_2, \mathbf{r}_3)] \times V_f(\mathbf{r}_2, t_2) V_f(\mathbf{r}_3, t_3), \quad \text{(C.19)}$$

where $\vec{K}^{(1)}(t_1, t_2, \mathbf{r}_2)$ is the linear response function for the combined variables z, ρ, and κ:

$$\vec{K}^{(1)}(t_1 - t_2, \mathbf{r}_2) = \mathcal{U}(t_1 - t_2)\tilde{\Phi}(\mathbf{r}_2)\vec{\psi}^{(0)}, \quad \text{(C.20)}$$

with the $2N(2N + 1) \times 1$ column vector $\vec{\Xi}_K(t_1 - t_2, t_1 - t_3; \mathbf{r}_2, \mathbf{r}_2')$ already been defined above in Eqs. (25) and (C.8). $\vec{\Xi}_K$ is derived from the vector $\vec{\Xi}(t)$ such that the components of the linear response vector $\vec{K}^{(1)}(t_1, t_2, \mathbf{r}_2)$, i.e., $\vec{K}_z^{(1)}(t_1, t_2, \mathbf{r}_2)$, $\vec{K}_\rho^{(1)}(t_1, t_2, \mathbf{r}_2)$, and $\vec{K}_\kappa^{(1)}(t_1, t_2, \mathbf{r}_2)$ defined in Eq. (C.9) replace, respectively, $z^{(1)}(t_1)$, $\rho^{(1)}(t_1)$, and $\kappa^{(1)}(t_1)$ in $\vec{\Xi}(t)$.

Using these results, the position-dependent time domain second-order response function for the combined variables z, ρ, and κ may finally be written as

$$\vec{K}^{(2)}(t, t_1, t_2, \mathbf{r}, \mathbf{r}_1, \mathbf{r}_2) = \tilde{\Upsilon}(\mathbf{r})[\vec{K}_I^{(2)} + \vec{K}_{II}^{(2)}], \quad \text{(C.21)}$$

where, after the change of variables $t_1 \longrightarrow \tau$, $t_2 \longrightarrow t_1$, and $t_3 \longrightarrow t_2$, $\vec{K}_I^{(2)}$ and $\vec{K}_{II}^{(2)}$ are given by

$$\vec{K}_I^{(2)}(t, t_1, t_2, \mathbf{r}_1, \mathbf{r}_2) = \mathcal{U}(t - t_1)\tilde{\Phi}(\mathbf{r}_1)\mathcal{U}(t_1 - t_2)\tilde{\Phi}(\mathbf{r}_2)\vec{\psi}^{(0)}, \quad \text{(C.22)}$$

$$\vec{K}_{II}^{(2)}(t, t_1, t_2, \mathbf{r}_1, \mathbf{r}_2) = \int_0^t d\tau \mathcal{U}(t - \tau)\vec{\Xi}_K(\tau - t_1, \tau - t_2, \mathbf{r}_1, \mathbf{r}_2). \quad \text{(C.23)}$$

The position-dependent second-order response functions for the condensate, the noncondensate density, and the correlation are given by summing over appropriate indices of the vector $\vec{K}^{(2)}$ (Eq. (C.21)):

$$K_z^{(2)}(t, t_1, t_2, \mathbf{r}, \mathbf{r}_1, \mathbf{r}_2) = \sum_{i=1}^{N} [\tilde{\Upsilon}(\mathbf{r})(\vec{K}_I^{(2)}(t, t_1, t_2, \mathbf{r}_1, \mathbf{r}_2) + \vec{K}_{II}^{(2)}(t, t_1, t_2, \mathbf{r}_1, \mathbf{r}_2))]_i, \quad \text{(C.24)}$$

$$K_\rho^{(2)}(t, t_1, t_2, \mathbf{r}, \mathbf{r}_1, \mathbf{r}_2) = \sum_{i=2N+1}^{2N+N^2} [\tilde{\Upsilon}(\mathbf{r})(\vec{K}_I^{(2)}(t, t_1, t_2, \mathbf{r}_1, \mathbf{r}_2) + \vec{K}_{II}^{(2)}(t, t_1, t_2, \mathbf{r}_1, \mathbf{r}_2))]_i, \quad \text{(C.25)}$$

$$K_\kappa^{(2)}(t, t_1, t_2, \mathbf{r}, \mathbf{r}_1, \mathbf{r}_2) = \sum_{i=2N+N^2+1}^{2N+2N^2} [\tilde{\Upsilon}(\mathbf{r})(\vec{K}_I^{(2)}(t, t_1, t_2, \mathbf{r}_1, \mathbf{r}_2) + \vec{K}_{II}^{(2)}(t, t_1, t_2, \mathbf{r}_1, \mathbf{r}_2))]_i. \quad \text{(C.26)}$$

where $\vec{K}_I^{(2)}$ and $\vec{K}_{II}^{(2)}$ are defined in Eqs. (C.22) and (C.23) and $\tilde{\Upsilon}$, $\mathcal{U}$, $\tilde{\Phi}$, and $\vec{\Xi}_K$ are defined in Eqs. (15), (23), (24), and (25) (or (C.8)), respectively.

C.3. Alternative Form for the Response Function

To discuss the response functions in the frequency domain and to understand the physical processes involved, it is useful to expand the response functions on the basis of the eigenvectors $\vec{\xi}_\nu$ of matrix $\mathcal{L}^{(2)}$ such that $\mathcal{L}^{(2)}\vec{\xi}_\nu = \omega_\nu \vec{\xi}_\nu$, with $\nu = 1, 2, \ldots, 2N(2N + 1)$. We define the Green's function

$$G_\nu(t - t') = \exp\left[-\frac{i}{\hbar}\omega_\nu(t - t')\right] \quad \text{(C.27)}$$

and the expansion coefficients μ_ν, $\eta_\nu(\mathbf{r})$, and $\delta_\nu(\mathbf{r})$ such that

$$\vec{\psi}^{(0)} = \sum_{\nu=1}^{2N(2N+1)} \mu_\nu \vec{\xi}_\nu, \quad \tilde{\Phi}(\mathbf{r})\vec{\xi}_{\nu'} = \sum_{\nu=1}^{2N(2N+1)} \eta_\nu(\mathbf{r})\vec{\xi}_\nu, \quad \text{and} \quad \tilde{\Upsilon}(\mathbf{r})\vec{\xi}_\nu = \sum_{\nu=1}^{2N(2N+1)} \delta_\nu(\mathbf{r})\vec{\xi}_\nu. \quad \text{(C.28)}$$

On the basis of these eigenstates, $\vec{\xi}_\nu$, the result is Eqs. (C.24)–(C.26) but with

$$\vec{K}_I^{(2)}(t, t_1, t_2, \mathbf{r}_1, \mathbf{r}_2) = \sum_{\nu=1}^{2N(2N+1)} \mathcal{K}_{I,\nu}^{(2)}(t, t_1, t_2, \mathbf{r}_1, \mathbf{r}_2)\vec{\xi}_\nu, \tag{C.29}$$

$$\vec{K}_{II}^{(2)}(t, t_1, t_2, \mathbf{r}_1, \mathbf{r}_2) = \sum_{\nu=1}^{2N(2N+1)} \mathcal{K}_{II,\nu}^{(2)}(t, t_1, t_2, \mathbf{r}_1, \mathbf{r}_2)\vec{\xi}_\nu, \tag{C.30}$$

where

$$\mathcal{K}_{I,\nu}^{(2)}(t, t_1, t_2, \mathbf{r}_1, \mathbf{r}_2) = \sum_{\nu',\nu''=1}^{2N(2N+1)} \eta_\nu(\mathbf{r}_1)\eta_{\nu'}(\mathbf{r}_2)G_\nu(t-t_1)\mu_{\nu''}G_{\nu'}(t_1-t_2), \tag{C.31}$$

and

$$\mathcal{K}_{II,\nu}^{(2)}(t, t_1, t_2, \mathbf{r}_1, \mathbf{r}_2) = \sum_{\nu',\nu''=1}^{2N(2N+1)} \int_0^t d\tau G_\nu(t-\tau) \times \mathcal{F}[\eta_{\nu'}(\mathbf{r}_1)\eta_{\nu''}(\mathbf{r}_2)\mu_{\nu'}\mu_{\nu''}G_{\nu'}(\tau-t_1)G_{\nu''}(\tau-t_2)]. \tag{C.32}$$

Here, $\mathcal{F}$ is the function given according to the expression for $\vec{\Xi}_K$ but written in terms of μ_ν, η_ν, and G_ν with $G_\nu(t-t')$, μ_ν, and η_ν as defined in Eqs. (C.27) and (C.28).

APPENDIX D

SECOND-ORDER SUSCEPTIBILITIES

In this appendix, we first summarize the final result for the second-order susceptibilities in Section D.1 and then provide a more detailed derivation in Section D.2. In the last subsection (Section D.3) of this appendix, we show an alternative form for the susceptibilities written on the basis of the eigenvectors of the Liouvillian.

D.1. Final Expression

The final result that we use for our numerical calculation for the condensate, the noncondensate density, and the noncondensate correlations are

$$K_z^{(2)}(-\Omega_1-\Omega_2; \Omega_1, \Omega_2, \mathbf{r}, \mathbf{r}_1, \mathbf{r}_2) = \sum_{i=1}^{N} [\tilde{\Upsilon}(\mathbf{r})(\vec{K}_I^{(2)}(\Omega_1, \Omega_2, \mathbf{r}_1, \mathbf{r}_2) + \vec{K}_{II}^{(2)}(\Omega_1, \Omega_2, \mathbf{r}_1, \mathbf{r}_2))]_i, \tag{D.1}$$

$$K_\rho^{(2)}(-\Omega_1-\Omega_2; \Omega_1, \Omega_2, \mathbf{r}, \mathbf{r}_1, \mathbf{r}_2) = \sum_{i=2N+1}^{2N+N^2} [\tilde{\Upsilon}(\mathbf{r})(\vec{K}_I^{(2)}(\Omega_1, \Omega_2, \mathbf{r}_1, \mathbf{r}_2) + \vec{K}_{II}^{(2)}(\Omega_1, \Omega_2, \mathbf{r}_1, \mathbf{r}_2))]_i, \tag{D.2}$$

$$K_\kappa^{(2)}(-\Omega_1-\Omega_2; \Omega_1, \Omega_2, \mathbf{r}, \mathbf{r}_1, \mathbf{r}_2) = \sum_{i=2N+N^2+1}^{2N+2N^2} [\tilde{\Upsilon}(\mathbf{r})(\vec{K}_I^{(2)}(\Omega_1, \Omega_2, \mathbf{r}_1, \mathbf{r}_2) + \vec{K}_{II}^{(2)}(\Omega_1, \Omega_2, \mathbf{r}_1, \mathbf{r}_2))]_i, \tag{D.3}$$

where

$$\vec{K}_I^{(2)}(\Omega_1, \Omega_2, \mathbf{r}, \mathbf{r}_1, \mathbf{r}_2) = -\frac{1}{4\pi^2}\tilde{\Upsilon}(\mathbf{r})\mathcal{U}(\Omega_1+\Omega_2)\tilde{\Phi}(\mathbf{r}_1)\mathcal{U}(\Omega_2)\tilde{\Phi}(\mathbf{r}_2)\vec{\psi}^{(0)}, \tag{D.4}$$

and

$$\vec{K}_{II}^{(2)}(\Omega_1, \Omega_2, \mathbf{r}, \mathbf{r}_1, \mathbf{r}_2) = -\frac{1}{8\pi^3 i}\tilde{\Upsilon}(\mathbf{r})\mathcal{U}(\Omega_1+\Omega_2)\vec{\Xi}_K(\Omega_1, \Omega_2, \mathbf{r}_1, \mathbf{r}_2). \tag{D.5}$$

Here, $\tilde{\Upsilon}(\mathbf{r})$ and $\tilde{\Phi}(\mathbf{r})$ are as defined in Eqs. (15) and (24) and

$$\mathcal{U}(\omega) \equiv \frac{1}{\omega - \mathcal{L}^{(2)} + i\epsilon}. \tag{D.6}$$

In addition, the vector $\vec{\Xi}_K(\Omega_1, \Omega_2, \mathbf{r}_1, \mathbf{r}_2)$ of Eq. (31) may be written as

$$\vec{\Xi}_K(\Omega_1, \Omega_2, \mathbf{r}_1, \mathbf{r}_2) = \left[\tilde{\mathcal{L}}_K, \tilde{\mathcal{L}}_K^*, \tilde{\mathcal{R}}_K, \tilde{\mathcal{K}}_K, \tilde{\mathcal{R}}_K^*, \tilde{\mathcal{K}}_K^*\right]^T \tag{D.7}$$

with the $N\times 1$ matrix $\tilde{\mathcal{L}}_K$ and $N^2\times 1$ matrices $\tilde{\mathcal{R}}_K$, $\tilde{\mathcal{K}}_K$ given as follows:

$$[\tilde{\mathcal{L}}_K]_i = \sum_{klr} V_{iklr}[[\vec{K}_z^{(1)*}(\Omega_1, \mathbf{r}_1)]_k z_l^{(0)}[\vec{K}_z^{(1)}(\Omega_2, \mathbf{r}_2)]_r + [\vec{K}_z^{(1)*}(\Omega_1, \mathbf{r}_1)]_k[\vec{K}_z^{(1)}(\Omega_2, \mathbf{r}_2)]_l z_r^{(0)} + z_k^{*(0)}[\vec{K}_z^{(1)}(\Omega_1, \mathbf{r}_1)]_l[\vec{K}_z^{(1)}(\Omega_2, \mathbf{r}_2)]_r + 2[\vec{K}_\rho^{(1)}(\Omega_1, \mathbf{r}_1)]_{lk}[\vec{K}_z^{(1)}(\Omega_2, \mathbf{r}_2)]_r \tag{D.8}$$

$$
\begin{aligned}
&+ [\vec{K}_\kappa^{(1)}(\Omega_1, \mathbf{r}_1)]_{kl}[\vec{K}_z^{(1)}(\Omega_2, \mathbf{r}_2)]_r],\\
&[\tilde{\mathcal{R}}_K]_{ij}\\
&= 2\sum_{rkl} V_{iklr}[\vec{K}_\rho^{(1)}(\Omega_1, \mathbf{r}_1)]_{rj}[\vec{K}_\rho^{(1)}(\Omega_2, \mathbf{r}_2)]_{kl}\\
&- V_{rklj}[\vec{K}_\rho^{(1)}(\Omega_1, \mathbf{r}_1)]_{kl}[\vec{K}_\rho^{(1)}(\Omega_2, \mathbf{r}_2)]_{ir}\\
&+ \sum_{rkl} V_{iklr}[\vec{K}_\kappa^{(1)}(\Omega_1, \mathbf{r}_1)]_{kl}[\vec{K}0_\kappa^{*(1)}(\Omega_2, \mathbf{r}_2)]_{rj}\\
&+ V_{rjkl}[\vec{K}_\kappa^{*(1)}(\Omega_1, \mathbf{r}_1)]_{kl}[\vec{K}_\kappa^{(1)}(\Omega_2, \mathbf{r}_2)]_{ir}\\
&+ 2\sum_{rkl} V_{iklr}[\vec{K}_z^{*(1)}(\Omega_1, \mathbf{r}_1)]_k[\vec{K}_z^{(1)}(\Omega_2, \mathbf{r}_2)]_l\rho_{rj}^{(0)}\\
&- V_{rklj}[\vec{K}_z^{*(1)}(\Omega_1, \mathbf{r}_1)]_k[\vec{K}_z^{(1)}(\Omega_2, \mathbf{r}_2)]_l\rho_{ir}^{(0)}\\
&+ 2\sum_{rkl} V_{iklr}[[\vec{K}_z^{*(1)}(\Omega_1, \mathbf{r}_1)]_k z_l^{(0)}\\
&+ z_k^{*(0)}[\vec{K}_z^{(1)}(\Omega_1, \mathbf{r}_1)]_l][\vec{K}_\rho^{(1)}(\Omega_2, \mathbf{r}_2)]_{rj}\\
&- V_{rklj}[[\vec{K}_z^{*(1)}(\Omega_1, \mathbf{r}_1)]_k z_l^{(0)} + z_k^{*(0)}[\vec{K}_z^{(1)}(\Omega_1, \mathbf{r}_1)]_l]\\
&\times [\vec{K}_\rho^{(1)}(\Omega_2, \mathbf{r}_2)]_{ir} + \sum_{rkl} V_{rjkl}[[\vec{K}_z^{(1)*}(\Omega_1, \mathbf{r}_1)]_k z_l^{*(0)}\\
&+ z_k^{*(0)}[\vec{K}_z^{*(1)}(\Omega_1, \mathbf{r}_1)]_l][\vec{K}_\kappa^{(1)}(\Omega_2, \mathbf{r}_2)]_{ir}\\
&- V_{irkl}[[\vec{K}_z^{(1)}(\Omega_1, \mathbf{r}_1)]_k z_l^{(0)} + z_k^{(0)}[\vec{K}_z^{(1)}(\Omega_1, \mathbf{r}_1)]_l]\\
&\times [\vec{K}_\kappa^{*(1)}(\Omega_2, \mathbf{r}_2)]_{rj} + \sum_{rkl} V_{rjkl}[\vec{K}_z^{(1)}(\Omega_1, \mathbf{r}_1)]_k\\
&\times [\vec{K}_z^{(1)}(\Omega_2, \mathbf{r}_2)]_l\kappa_{ir}^{(0)}\\
&- V_{irkl}[\vec{K}_z^{(1)}(\Omega_1, \mathbf{r}_1)]_k[\vec{K}_z^{(1)}(\Omega_2, \mathbf{r}_2)]_l\kappa_{rj}^{*(0)},
\end{aligned}
\tag{D.9}
$$

$$
\begin{aligned}
&[\tilde{\mathcal{H}}_K]_{ij}\\
&= 2\sum_{rkl} V_{iklr}[\vec{K}_\kappa^{(1)}(\Omega_1, \mathbf{r}_1)]_{rj}[\vec{K}_\rho^{(1)}(\Omega_2, \mathbf{r}_2)]_{lk}\\
&+ V_{rklj}[\vec{K}_\rho^{(1)}(\Omega_1, \mathbf{r}_1)]_{kl}[\vec{K}_\kappa^{(1)}(\Omega_2, \mathbf{r}_2)]_{ir}\\
&+ \sum_{rkl} V_{irkl}[\vec{K}_\kappa^{(1)}(\Omega_1, \mathbf{r}_1)]_{kl}[\vec{K}_\rho^{(1)*}(\Omega_2, \mathbf{r}_2)]_{rj}\\
&+ V_{rjkl}[\vec{K}_\kappa^{(1)}(\Omega_1, \mathbf{r}_1)]_{kl}[\vec{K}_\rho^{(1)}(\Omega_2, \mathbf{r}_2)]_{ir}\\
&+ 2\sum_{rkl} V_{iklr}[\vec{K}_z^{*(1)}(\Omega_1, \mathbf{r}_1)]_k[\vec{K}_z^{(1)}(\Omega_2, \mathbf{r}_2)]_l\kappa_{rj}^{(0)}\\
&+ V_{rklj}[\vec{K}_z^{(1)}(\Omega_1, \mathbf{r}_1)]_k[\vec{K}_z^{*(1)}(\Omega_2, \mathbf{r}_2)]_l\kappa_{ir}^{(0)}\\
&+ 2\sum_{rkl} V_{iklr}[[\vec{K}_z^{(1)*}(\Omega_1, \mathbf{r}_1)]_k z_l^{0(0)}\\
&+ z_k^{*(0)}[\vec{K}_z^{(1)}(\Omega_1, \mathbf{r}_1)]_l][\vec{K}_\kappa^{(2)}(\Omega_1, \mathbf{r}_2)]_{rj}\\
&+ V_{rklj}[[\vec{K}_z^{(1)}(\Omega_1, \mathbf{r}_1)]_k z_l^{*(0)}\\
&+ z_k^{(0)}[\vec{K}_z^{*(1)}(\Omega_1, \mathbf{r}_1)]_l][\vec{K}_\kappa^{(1)}(\Omega_2, \mathbf{r}_2)]_{ir}\\
&+ \sum_{rkl} V_{rjkl}[[\vec{K}_z^{(1)}(\Omega_1, \mathbf{r}_1)]_k z_l^{(0)}\\
&+ z_k^{(0)}[\vec{K}_z^{(1)}(\Omega_1, \mathbf{r}_1)]_l][\vec{K}_\rho^{(1)}(\Omega_2, \mathbf{r}_2)]_{ir}\\
&+ V_{irkl}[[\vec{K}_z^{(1)}(\Omega_1, \mathbf{r}_1)]_k z_l^{(0)}\\
&+ z_k^{(0)}[\vec{K}_z^{(1)}(\Omega_1, \mathbf{r}_1)]_l][\vec{K}_\rho^{*(1)}(\Omega_2, \mathbf{r}_2)]_{rj}\\
&+ \sum_{rkl} V_{rjkl}[\vec{K}_z^{(1)}(\Omega_1, \mathbf{r}_1)]_k[\vec{K}_z^{(1)}(\Omega_2, \mathbf{r}_2)]_l\rho_{ir}^{(0)}\\
&+ V_{irkl}[\vec{K}_z^{(1)}(\Omega_1, \mathbf{r}_1)]_k[\vec{K}_z^{(1)}(\Omega_2, \mathbf{r}_2)]_l\rho_{rj}^{*(0)}\\
&+ \sum_{kl} V_{ijkl}[\vec{K}_z^{(1)}(\Omega_1, \mathbf{r}_1)]_k[\vec{K}_z^{(1)}(\Omega_2, \mathbf{r}_2)]_l.
\end{aligned}
\tag{D.10}
$$

Similar to Eq. (C.9) above, the quantities $\vec{K}_z^{(1)}(\Omega_i, \mathbf{r}_i)$, $\vec{K}_\rho^{(1)}(\Omega_i, \mathbf{r}_i)$, and $\vec{K}_\kappa^{(1)}(\Omega_i, \mathbf{r}_i)$ used in Eqs. (D.8)–(D.10) are defined as

$$
\vec{K}_\alpha^{(1)}(\Omega_i, \mathbf{r}_i) = \mathcal{U}^{(\alpha)}(\Omega_i)\tilde{\Phi}(\mathbf{r}_i)\vec{\psi}^{(0)}, \tag{D.11}
$$

where $\alpha = z, \rho, \kappa$, and $i = 1, 2$. $\mathcal{U}^{(\alpha)}(\Omega_i)$ are the submatrices of $\mathcal{U}(\Omega_i)$ defined in Eq. (32) such that

$$
\begin{aligned}
\mathcal{U}(\Omega_i) = [&\mathcal{U}^{(z)}(\Omega_i), \mathcal{U}^{(z)*}(\Omega_i),\\
&\mathcal{U}^{(\rho)}(\Omega_i), \mathcal{U}^{(\kappa)}(\Omega_i), \mathcal{U}^{(\rho)*}(\Omega_i), \mathcal{U}^{(\kappa)*}(\Omega_i)]^T,
\end{aligned}
\tag{D.12}
$$

where $\mathcal{U}^{(z)}(\Omega_i)$ is an $N \times 2N(2N + 1)$ submatrix while $\mathcal{U}^{(\gamma)}(\Omega_i)$, $\gamma = \rho, \kappa, \rho^*, \kappa^*$ is an $N^2 \times 2N(2N + 1)$ submatrix such that the submatrix $\mathcal{U}^{(z)}(\Omega_i)$ is stacked on top of submatrix $\mathcal{U}^{(z)*}(\Omega_i)$, which, in turn, is stacked on top of submatrices $\mathcal{U}^{(\gamma)}(\Omega_i)$. It is to be noted that, as with

the time domain example discussed above, $\vec{K}_\alpha^{(1)}(\Omega_i, \mathbf{r}_i)$ as defined here are $N \times 1$ and $N^2 \times 1$ vectors, not scalar quantities obtained by integrating the scalar function $K_\alpha^{(1)}(\Omega_i, \mathbf{r}, \mathbf{r}_i)$ over $\mathbf{r}$.

D.2. Derivation

The second-order response function in frequency is given by the Fourier transform of the time domain counterpart:

$$\vec{K}^{(2)}(\Omega, \Omega_1, \Omega_2, \mathbf{r}, \mathbf{r}_1, \mathbf{r}_2) = \int_0^\infty dt dt_1 \tilde{\Upsilon}(\mathbf{r})[\vec{K}_I^{(2)} + \vec{K}_{II}^{(2)}] \times \exp(i\Omega t + i\Omega_1 t_1 + i\Omega_2 t_2) \quad \text{(D.13)}$$

$$= \tilde{\Upsilon}(\mathbf{r})[\vec{K}_I^{(2)}(\Omega, \Omega_1, \Omega_2, \mathbf{r}_1, \mathbf{r}_2) + \vec{K}_{II}^{(2)}(\Omega, \Omega_1, \Omega_2, \mathbf{r}_1, \mathbf{r}_2)], \quad \text{(D.14)}$$

where $\vec{K}_I^{(2)}(\Omega, \Omega_1, \Omega_2, \mathbf{r}_1, \mathbf{r}_2)$ and $\vec{K}_{II}^{(2)}(\Omega, \Omega_1, \Omega_2, \mathbf{r}_1, \mathbf{r}_2)$ are the Fourier transforms of the time domain expressions (Eqs. (C.22), (C.23)).

Using the fact that the matrices $\mathcal{U}(t - t_1)$ are the Green's functions with an implicit Heaviside step function in time, i.e., $\mathcal{U}(t - t_1) \equiv \theta(t - t_1)\mathcal{U}(t - t_1)$ such that

$$\theta(t)\mathcal{U}(t) = -\frac{1}{2\pi i}\int_{-\infty}^{\infty} d\omega \frac{1}{\omega - \mathcal{L}^{(2)} + i\epsilon}\exp(-i\omega t) \quad \text{(D.15)}$$

$$= \int_{-\infty}^{\infty} d\omega \mathcal{U}(\omega)\exp(-i\omega t), \quad \text{(D.16)}$$

we have

$$\vec{K}_I^{(2)}(\Omega, \Omega_1, \Omega_2, \mathbf{r}_1, \mathbf{r}_2) = -\frac{1}{4\pi^2}\int_{-\infty}^{\infty} d\omega d\omega' \times \tilde{\Upsilon}(\mathbf{r})\mathcal{U}(\omega)\tilde{\Phi}(\mathbf{r}_1)\mathcal{U}(\omega')\tilde{\Phi}(\mathbf{r}_2)\vec{\psi}^{(0)}\delta(\Omega - \omega) \times \delta(\Omega_1 + \omega - \omega')\delta(\Omega_2 + \omega'). \quad \text{(D.17)}$$

This implies that $\omega' = -\Omega_2$, $\omega = -\Omega_1 - \Omega_2$, and $\Omega = -\Omega_1 - \Omega_2$:

$$K_I^{(2)}(-\Omega_1 - \Omega_2; \Omega_1, \Omega_2, \mathbf{r}, \mathbf{r}_1, \mathbf{r}_2) = -\frac{1}{4\pi^2}\tilde{\Upsilon}(\mathbf{r})\mathcal{U}(\Omega_1 + \Omega_2)\tilde{\Phi}(\mathbf{r}_1)\mathcal{U}(\Omega_2)\tilde{\Phi}(\mathbf{r}_2)\vec{\psi}^{(0)}. \quad \text{(D.18)}$$

In addition, we have

$$\vec{K}_{II}^{(2)}(\Omega, \Omega_1, \Omega_2, \mathbf{r}, \mathbf{r}_1, \mathbf{r}_2) = -\frac{1}{8\pi^3 i}\int_{-\infty}^{\infty} d\omega d\omega' d\omega'' \times \tilde{\Upsilon}(\mathbf{r})\mathcal{U}(\omega)\vec{\vec{\Xi}}_K(\omega', \omega'', \mathbf{r}_1, \mathbf{r}_2)\delta(\omega - \omega' - \omega'') \times \delta(\Omega - \omega)\delta(\Omega_1 + \omega')\delta(\Omega_2 + \omega''). \quad \text{(D.19)}$$

We are able to write the Fourier transform for $\vec{\vec{\Xi}}_K(t)$ in Eq. (D.19) since the function $\vec{\vec{\Xi}}_K(t)$ is made up of terms which are simply products of two Green's functions at different times. Equation (D.19) implies $\omega' = -\Omega_1$, $\omega'' = -\Omega_2$, $\omega = \omega' + \omega'' = -\Omega_1 - \Omega_2$, $\Omega = \omega$, so that

$$K_{II}^{(2)}(-\Omega_1 - \Omega_2; \Omega_1, \Omega_2, \mathbf{r}, \mathbf{r}_1, \mathbf{r}_2) = -\frac{1}{8\pi^3 i}\tilde{\Upsilon}(\mathbf{r})\mathcal{U}(\Omega_1 + \Omega_2)\vec{\vec{\Xi}}_K(\Omega_1, \Omega_2, \mathbf{r}_1, \mathbf{r}_2), \quad \text{(D.20)}$$

where $\vec{\vec{\Xi}}_K(\Omega_1, \Omega_2, \mathbf{r}_1, \mathbf{r}_2)$ is as already given in Eq. (D.10).

As for the time domain calculations, the susceptibilities for the condensate, the noncondensate density, and the noncondensate correlations are obtained by summing over the appropriate indices:

$$K_z^{(2)}(-\Omega_1 - \Omega_2; \Omega_1, \Omega_2, \mathbf{r}, \mathbf{r}_1, \mathbf{r}_2) = \sum_{i=1}^{N}[\tilde{\Upsilon}(\mathbf{r})(\vec{K}_I^{(2)}(\Omega_1, \Omega_2, \mathbf{r}_1, \mathbf{r}_2) + \vec{K}_{II}^{(2)}(\Omega_1, \Omega_2, \mathbf{r}_1, \mathbf{r}_2))]_i, \quad \text{(D.21)}$$

$$K_\rho^{(2)}(-\Omega_1 - \Omega_2; \Omega_1, \Omega_2, \mathbf{r}, \mathbf{r}_1, \mathbf{r}_2) = \sum_{i=2N+1}^{2N+N^2}[\tilde{\Upsilon}(\mathbf{r})(\vec{K}_I^{(2)}(\Omega_1, \Omega_2, \mathbf{r}_1, \mathbf{r}_2) + \vec{K}_{II}^{(2)}(\Omega_1, \Omega_2, \mathbf{r}_1, \mathbf{r}_2))]_i, \quad \text{(D.22)}$$

$$K_\kappa^{(2)}(-\Omega_1 - \Omega_2; \Omega_1, \Omega_2, \mathbf{r}, \mathbf{r}_1, \mathbf{r}_2) = \sum_{i=2N+N^2+1}^{2N+2N^2}[\tilde{\Upsilon}(\mathbf{r})(\vec{K}_I^{(2)}(\Omega_1, \Omega_2, \mathbf{r}_1, \mathbf{r}_2) + \vec{K}_{II}^{(2)}(\Omega_1, \Omega_2, \mathbf{r}_1, \mathbf{r}_2))]_i. \quad \text{(D.23)}$$

D.3. Alternative Form for the Susceptibility

As before, expanding in the eigenstate basis $\vec{\xi}_\nu$ that we introduced in Eq. (C.28), we may write the suscep-

tibility in a more useful form. The result is Eqs. (D.21)–(D.23) but with

$$\vec{K}_I^{(2)}(-\Omega_1-\Omega_2;\,\Omega_1,\Omega_2,\mathbf{r}_1,\mathbf{r}_2) = \sum_{\nu=1}^{2N(2N+1)} \mathcal{H}_{I,\nu}^{(2)}(-\Omega_1-\Omega_2;\,\Omega_1,\Omega_2,\mathbf{r}_1,\mathbf{r}_2)\vec{\xi}_\nu, \quad \text{(D.24)}$$

$$\vec{K}_{II}^{(2)}(-\Omega_1-\Omega_2;\,\Omega_1,\Omega_2,\mathbf{r}_1,\mathbf{r}_2) = \sum_{\nu=1}^{2N(2N+1)} \mathcal{H}_{II,\nu}^{(2)}(-\Omega_1-\Omega_2;\,\Omega_1,\Omega_2,\mathbf{r}_1,\mathbf{r}_2)\vec{\xi}_\nu, \quad \text{(D.25)}$$

where

$$\mathcal{H}_{I,\nu}^{(2)}(-\Omega_1-\Omega_2;\,\Omega_1,\Omega_2,\mathbf{r}_1,\mathbf{r}_2) = -\frac{1}{4\pi^2}\sum_{\nu',\nu''=1}^{2N(2N+1)} \frac{\eta_\nu(\mathbf{r}_1)\eta_{\nu'}(\mathbf{r}_2)\mu_{\nu''}}{(\Omega_1+\Omega_2-\omega_\nu+i\epsilon)(\Omega_2-\omega_{\nu'}+i\epsilon)}. \quad \text{(D.26)}$$

Since no additional information is gained by listing all the terms in $\mathcal{H}_{II,\nu}^{(2)}(-\Omega_1-\Omega_2;\,\Omega_1,\Omega_2,\mathbf{r}_1,\mathbf{r}_2)$, we simply note that, in the eigenstate basis, the typical term in $\mathcal{H}_{II,\nu}^{(2)}$ has the structure

$$\sum_{\nu'\nu''=1}^{2N(2N+1)} \frac{\eta_\nu(\mathbf{r}_1)\eta_{\nu'}(\mathbf{r}_2)\mu_{\nu''}}{(\Omega_1+\Omega_2-\omega_\nu+i\epsilon)(\Omega_2-\omega_\nu+i\epsilon)(\Omega_2-\omega_{\nu'}+i\epsilon)}, \quad \text{(D.27)}$$

as is to be expected from Eqs. (D.10) and (D.20). μ_ν and η_ν are as given in Eq. (C.28).

REFERENCES

1. A. Griffin, D. W. Snoke, and S. Stringari, *Bose–Einstein Condensation* (Cambridge Univ. Press, New York, 1995).
2. R. E. Prange and S. M. Girvin, *The Quantum Hall Effect* (Springer, New York, 1987).
3. S. Mukamel, *Principles of Nonlinear Optical Spectroscopy* (Oxford Univ. Press, New York, 1999).
4. I. E. Perakis and T. V. Shahbazyan, Int. J. Mod. Phys. B **13**, 869 (1999); I. E. Perakis and T. V. Shahbazyan, Surf. Sci. Rep. **40**, 3 (2000).
5. M. Trippenbach, Y. B. Band, and P. S. Julienne, Phys. Rev. A **62**, 023608 (2000).
6. V. Chernyak, S. Choi, and S. Mukamel, Phys. Rev. A **67**, 053604 (2003).
7. S. Choi, V. Chernyak, and S. Mukamel, Phys. Rev. A **67**, 043602 (2003).
8. P. Ring and P. Schuck, *The Nuclear Many-body Problem* (Springer, New York, 1980).
9. J.-P. Blaizot and G. Ripka, *Quantum Theory of Finite Systems* (MIT Press, Cambridge, MA, 1986).
10. A. Griffin, Phys. Rev. B **53**, 9341 (1996).
11. N. P. Proukakis and K. Burnett, J. Res. Natl. Inst. Stand. Technol. **101**, 457 (1996).
12. Y. Castin and R. Dum, Phys. Rev. A **57**, 3008 (1998); Phys. Rev. Lett. **79**, 3553 (1997).
13. L. P. Kandanoff and G. Baym, *Quantum Statistical Mechanics* (Benjamin, New York, 1962).
14. P. C. Hohenberg and P. C. Martin, Ann. Phys. (N.Y.) **34**, 291 (1965).
15. C. W. Gardiner and P. Zoller, Phys. Rev. A **55**, 2902 (1997); D. Jaksch, C. W. Gardiner, and P. Zoller, Phys. Rev. A **56**, 575 (1997); C. W. Gardiner and P. Zoller, Phys. Rev. A **58**, 536 (1998); D. Jaksch, C. W. Gardiner, K. M. Gheri, and P. Zoller, Phys. Rev. A **58**, 1450 (1998); C. W. Gardiner and P. Zoller, Phys. Rev. A **61**, 033601 (2000).
16. E. Zaremba, T. Nikuni, and A. Griffin, J. Low Temp. Phys. **116**, 277 (1999).
17. R. Walser, J. Williams, J. Cooper, and M. Holland, Phys. Rev. A **59**, 3878 (1999); R. Walser, J. Cooper, and M. Holland, Phys. Rev. A **63**, 013 607 (2000); J. Wachter, R. Walser, J. Cooper, and M. Holland, Phys. Rev. A **64**, 053612 (2001).
18. B. Jackson and E. Zaremba, Phys. Rev. Lett. **88**, 180 402 (2002).
19. W. Krauth, Phys. Rev. Lett. **77**, 3695 (1996).
20. D. M. Ceperley, Rev. Mod. Phys. **71**, S438 (1999).
21. M. J. Steel, M. K. Olsen, L. I. Plimak, *et al.*, Phys. Rev. A **58**, 4824 (1998).
22. P. D. Drummond and J. F. Corney, Phys. Rev. A **60**, R2661 (1999).
23. I. Carusotto, Y. Castin, and J. Dalibard, Phys. Rev. A **63**, 023606 (2001).
24. V. Chernyak and S. Mukamel, J. Chem. Phys. **104**, 444 (1996); S. Tretiak, V. Chernyak, and S. Mukamel, J. Am. Chem. Soc. **119**, 11408 (1997); S. Tretiak and S. Mukamel, Chem. Rev. **102**, 3171 (2002).
25. M. R. Geller and D. Loss, cond-mat/9709074 (1997).
26. S. C. Zhang, T. H. Hansson, and S. Kivelson, Phys. Rev. Lett. **62**, 82 (1989).
27. A. Lopez and E. Fradkin, Phys. Rev. B **44**, 5246 (1991).

28. H. F. Meng, Phys. Rev. B **49**, 1205 (1994).
29. R. B. Laughlin, Phys. Rev. Lett. **50**, 1395 (1983).
30. J. K. Jain, Phys. Rev. Lett. **63**, 199 (1989).
31. B. I. Halperin, P. A. Lee, and N. Read, Phys. Rev. B **47**, 7312 (1993).
32. N. A. Zimbovskaya and J. L. Birman, Phys. Rev. B **60**, 16 762 (1999).
33. N. A. Zimbovskaya and J. L. Birman, Int. J. Mod. Phys. B **13**, 859 (1999).
34. D. S. Jin, J. R. Ensher, M. R. Matthews, *et al.*, Phys. Rev. Lett. **77**, 420 (1996).
35. M.-O. Mewes, M. R. Andrews, N. J. van Druten, *et al.*, Phys. Rev. Lett. **77**, 416 (1996).
36. F. Chatelin, *Eigenvalues of Matrices* (Wiley, New York, 1993); V. Chernyak, M. F. Schulz, and S. J. Mukamel, J. Chem. Phys. **113**, 36 (2000).
37. G. B. Arfken and H. J. Weber, *Mathematical Methods for Physicists*, 4th ed. (Academic, San Diego, 1995).
38. G. H. Golub and C. F. Van Loan, *Matrix Computations* (Hopkins Univ. Press, Baltimore, 1983).
39. A. M. Perelomov, *Generalized Coherent States and Their Applications* (Springer, New York, 1986).
40. V. Chernyak and S. Mukamel, J. Chem. Phys. **111**, 4383 (1999).
41. T.-L. Ho, Phys. Rev. Lett. **87**, 060403 (2001); V. Schweikhard, I. Coddington, P. Engels, *et al.*, cond-mat/0308582 (2003); E. Akkermans and S. Ghosh, cond-mat/0307418 (2003).